Evaluating the use of surface source banking to accelerate Monte Carlo transport simulations of far-field particle fluxes

by

Eleni T. Mowery

Submitted to the
Department of Nuclear Science and Engineering

In Partial Fulfillment of the Requirements for the Degree of

BACHELOR OF SCIENCE IN ENGINEERING
as recommended by the Department of Nuclear Science and Engineering

at the

MASSACHUSETTS INSTITUTE OF TECHNOLOGY

May 2025

Authored by: Eleni Mowery
Department of Nuclear Engineering
May 13, 2025

Certified by: Benoit Forget
Department Head and KEPCO Professor of Nuclear Science and Engineering
Thesis Supervisor

Accepted by: Jacopo Buongiorno
Battelle Energy Alliance Professor in Nuclear Science and Engineering
Undergraduate Officer, Department of Nuclear Science and Engineering

Evaluating the use of surface source banking to accelerate Monte Carlo transport simulations of far-field particle fluxes

by

Eleni T. Mowery

Submitted to the Department of Nuclear Science and Engineering on May 13, 2025
In partial fulfillment of the requirements for the degree of
Bachelor of Science in Engineering as Recommended by the Department of Nuclear Science and Engineering

ABSTRACT

In order to enhance the verifiability and usability of surface source banking as a far-field flux and dose simulation acceleration method for Monte Carlo neutron transport codes, two surface source stationarity criteria were developed and evaluated. Surface sources were considered defined, or an accurate proxy for fission sources in eigenvalue simulations once enough particles have been banked such that these criteria were met. One criterion utilizes multi-dimensional Shannon entropy to indicate the stationarity of the surface source in physical space and energy. The other criterion uses functional expansions to track the stationarity of Legendre coefficients associated with spatially-dependent banked effective neutron reaction rates with different Z materials. The completion of a test case with an OpenMC model of an MK2 TRIGA facility indicated agreement between the two criteria. Effects of oversampling a surface source that met the stationarity criteria, as well as potential limitations of the surface source banking method itself were also examined via the test case.

Thesis Supervisor: Benoit Forget
Title: Department Head and KEPCO Professor of Nuclear Science and Engineering

Contents

List of Figures

List of Tables

1. Introduction

OpenMC[1] is an extensively-benchmarked, open source Monte Carlo neutron and photon transport code. OpenMC is highly capable, and has recently begun to be used for many aspects of advanced nuclear reactor design. Its open source status readily expands the accessibility of nuclear research and design, which is especially of relevance for large-scale research thrusts that foster collaboration between government, industry, and academic institutions. One such research thrust is the US government's recently intensified interest in advanced nuclear reactors to serve as high-performance propulsion and power systems for near-term cislunar and interplanetary space missions[2]. To meet this need, NASA is looking to researchers and contractors from a wide range of institutions to contribute to the design and evaluation of these nuclear systems[2]. OpenMC has proven efficacy in predicting several parameters essential to the core design and thermal hydraulics modeling required for this effort, such as criticality, feedback coefficients, kinetics, and spatially-dependent particle flux and heat deposition.

Recent releases of OpenMC include built-in surface-source methods that can accelerate the far-field flux simulations. These simulations are needed for informing the design of nuclear systems where high-fidelity shielding design is of high importance, like space nuclear technology, where shielding mass is strictly limited to ensure launchability and in-space performance of propulsive systems. However, there is currently no established means of determining when the use of surface sources is indicated, or when a surface source can be considered correctly defined. This uncertainty severely limits the usability of tools like OpenMC towards the design of shielded systems subject to strict regulatory and safety standards, and needs to be resolved prior to its wider use in such high-fidelity applications.

To resolve this need, this work will entail the development of a hybrid-approach surface source convergence criteria set that can be implemented in OpenMC, enabling higher-accuracy modeling of far-field neutron and particle fluxes. This will require the development of a mathematical and computational framework for quantifying the convergence of the distribution of particle states (position, trajectory, energy) as they are banked on a surface source surrounding the active region of a reactor model. This framework will then be applied to a simple reactor model using a large number of particles and neutron generations to determine when different moments of the functions describing the distribution of these quantities stabilize. From the analysis of this data, a set of concrete surface source stationarity conditions will be determined.

After these stationarity conditions have been identified and used to generate surface source banks for a sample reactor problem, the surface source banks will be used in fixed-source calculations to determine the accuracy and real computational acceleration potential of the surface source banking method. Multiple test cases will be run to determine the limitations of the method, as well as the effects of oversampling a surface source bank.

These results, along with the establishment of said stationarity conditions and the associated methodology used to find them has the potential to enhance both the speed and accuracy of OpenMC's far-field flux simulation capability, with the expectation of enabling it to perform to regulatory and industry standards for nuclear shielding design and evaluation.

The convergence quantification methods utilized by this thesis will be informed by extensive existing research on quantifying the spatial convergence of fission sources via entropy-based approaches[3,4]. This thesis will also build upon recent research on the use of functional expansions for expressing Monte Carlo neutron transport results as continuous functions, rather than discrete results[5], for the more efficient determination of neutron power distributions in a reactor core. This concept was most recently explored by Han, Z (2020), as a means of more efficiently producing fine-resolution results for coupling with thermal hydraulic codes. A major intent of this thesis research is to demonstrate that this methodology can also be applied towards the measurement of neutron state distributions as they are banked on a surface. Ultimately, the aim of this thesis research is to demonstrate the potential applicability of both functional expansion-based source determination methods towards quantifying not only the spatial distribution of particles for power profiles and fission sources, but also their energy distributions. If successful, the use of these methods to establish confidence in banked source definition would extend the usability of this technique to far-field flux modeling, and potentially other applications in reactor physics.

2. Background

2.1: Overview

Monte Carlo-based neutron and photon transport codes are used to stochastically solve both eigenvalue/criticality and simulation/fixed source problems for the design and evaluation of nuclear systems. The computational cost of these simulations increases linearly with the number of particles being simulated. For situations where only particle fluxes in the active reactor core and nearby structures are of interest, particle density per total particles simulated is high, and thus, the uncertainty associated with these fluxes is low. However, for shielding problems, where fluxes in regions spatially far from the active core region need to be modeled with high precision, the vast majority of particles produced via fission and decay processes in the core are absorbed prior to reaching a shielded region of interest. As a result, density of particles tracked in these regions per total particles simulated is low, and the stochastic uncertainty on the far-field fluxes of interest is high, making this process computationally inefficient.

Fig. 1 demonstrates this problem with a neutron flux incident upon a 1D graphite slab. As with a more complex geometry or neutron source, flux is attenuated exponentially at a rate determined by the macroscopic absorption and total neutron cross sections of the medium it is traveling through. Uncertainty on the flux measurements is proportional to the inverse square

root of the flux, and increases significantly with distance from the neutron source. One should note that this attenuation is still significant in a pure graphite (weakly-absorbing) medium.

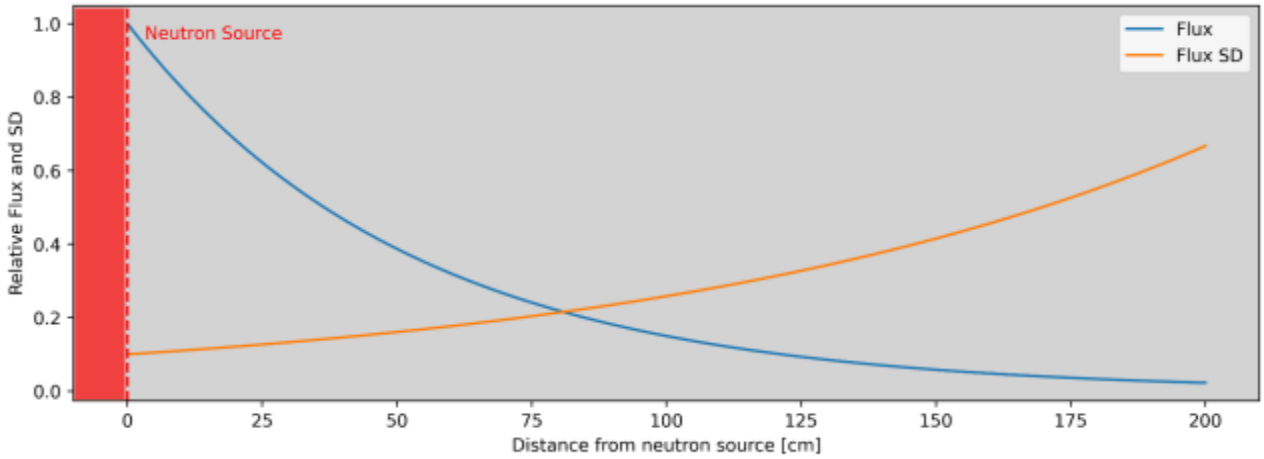

Figure 1. Demonstration of neutron flux attenuation and uncertainty in a 1D graphite slab

This issue is especially prevalent for space nuclear applications, which have recently become of increased interest to government and industry groups[2]. In these applications, distances between the active core(s) and humans and/or sensitive electronics can be vast. One such concept, the Copernicus B Mars Transport Vehicle (**Fig. 2**) is designed with 90m between the active nuclear cores of its engines and the human habitat module.

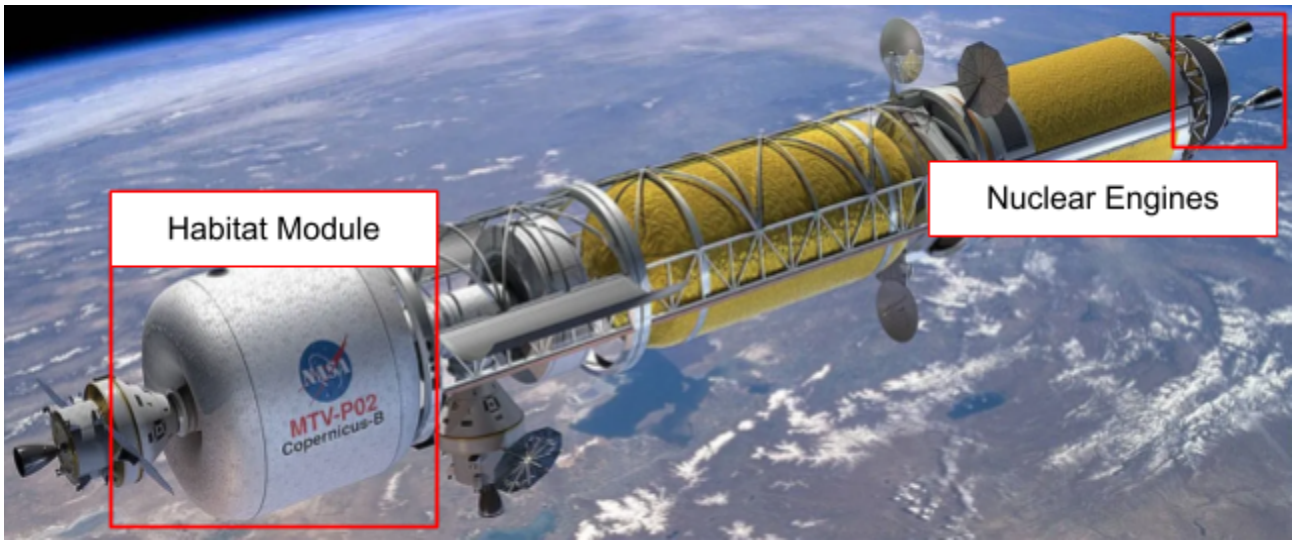

Figure 2. Copernicus B Mars Transport Vehicle conceptual design

Source-banking is a variance reduction technique that resolves this inefficiency for shielding problems by reducing runtime in the iterative design process. Instead of modeling particles within the active core in order to then track the transport of the small percentage that ultimately

survive to the far-field regions of interest, the computationally-intensive modeling of the core itself is bypassed by approximating the core as a predetermined bank of particles. The particle bank is created by simulating the active core and its immediate surroundings, and storing particles that cross a surface drawn around the active region. This source bank can then be used as a proxy for the core itself, greatly reducing unnecessary computational cost for shielding calculations. In **Sec. 5**, this capability is demonstrated using an OpenMC model of an MK2 TRIGA reactor, and achieved significant improvement in the precision of far-field flux predictions relative to computational time.

For a source bank to accurately represent a reactor core, it is essential to bank enough particles to reflect an accurate distribution of particle energy, angle, and spatial density on the banking surface. Prior to this work, there was no means of determining when enough particles have been banked—it was customary to conservatively simulate and bank extremely high particle counts, using significant computational resources without a means of quantifying how well the resulting source is defined. Now, the means of quantifying source convergence developed in this work could serve as a measure of the ultimate "definition" of the source, and provide an indication of when a minimum number of particles have been banked for the source bank to serve as an adequate proxy for the active core.

In summary, quantifying the convergence of particles banked on a surface source required not only confidence in their position, as would be the case for a fission source or power shape determination, but also their trajectory and energy. Accurate definition of all three relevant variables defining a particle state is critical, as particle trajectory and energy have a significant effect on the results of future far-field flux simulations that utilize the banked source. This work both develops and tests a methodology for quantifying the convergence of the distribution for each variable, enabling higher confidence in the accuracy of shielding simulation results produced accelerated via source-banking methods.

2.2 Oversampling banked source sites

It is important to consider the implications of oversampling a surface source when using it in fixed source calculations after it has been banked. In this work, the performance of banked surface sources is first evaluated with the imposed limitation that particles from the surface source will be simulated a maximum of once each to avoid oversampling bias. At present, limited duplicate sampling cannot be avoided, as OpenMC running in fixed source mode chooses particles from the surface bank randomly with replacement—particles are not removed from the bank after being simulated.

This limitation is significant, as in an eigenvalue Monte Carlo simulation of a reactor core, even if the surface source mesh has been drawn close to the boundary of the fissionable area of

the core, relatively few particles out of the total simulated will cross it and be stored on the particle bank. Additionally, an exceptionally large surface source file presents storage and analysis challenges. A fixed source simulation utilizing all particles within the bank once without resampling will run in a fraction of the time that the eigenvalue case ran in, but not allow for simulating comparatively further-field regions of the core. Oversampling the surface source—running the fixed source calculation with enough particles such that individual particles in the source bank are randomly chosen more than once—increases the probability that enough particles will not be attenuated prior to reaching regions far from the active core.

This allows for better variance on far-field flux predictions, but also means that the same particle starting site will be chosen multiple times, introducing bias. However, this bias is limited to solely the source sites themselves—oversampling a source bank does not result in particles sampled from the same site having identical simulated histories. By default, when particles are sampled from the surface source, they are assigned a unique random number seed different from that of the particle originally banked, so their histories beyond their initial trajectory are unique.

Should a surface source be large enough and proven to be representative of the core, the bias introduced by oversampling is likely small enough such that the results of the fixed source calculations are still useful from a dose and shielding calculation perspective. Analysis in **Sec. 5.3**, where an oversampled surface source is compared against a much higher particle count eigenvalue case, supports this prediction.

While the accuracy of these results is costly to verify, (and not immediately apparent, as OpenMC's measure of variance does not account for correlations from oversampling a source source) the oversampled fixed source case is able to simulate far-field regions of the core where not a single particle was simulated during the eigenvalue case where the source particles were banked.

Fig. 3 demonstrates this principle with a 2D neutron flux plot of a reactor core. The active core is overlaid with red, and the surface source is a cylindrical mesh surrounding the active core outlined with orange. The surface source was banked during an eigenvalue case (right), and utilized during a fixed source case (left), where each of the particles banked were randomly sampled and simulated an average of 100 times each, such that regions not reached by particle flux in the source banking eigenvalue case are simulated. The statistical error plotted is the standard deviation of flux in a mesh cell divided by its nominal magnitude. In **Sec. 5.3**, it will be shown that oversampling a surface source created in a limited particle count eigenvalue case produces flux density predictions in alignment with that of a much higher particle count eigenvalue case.

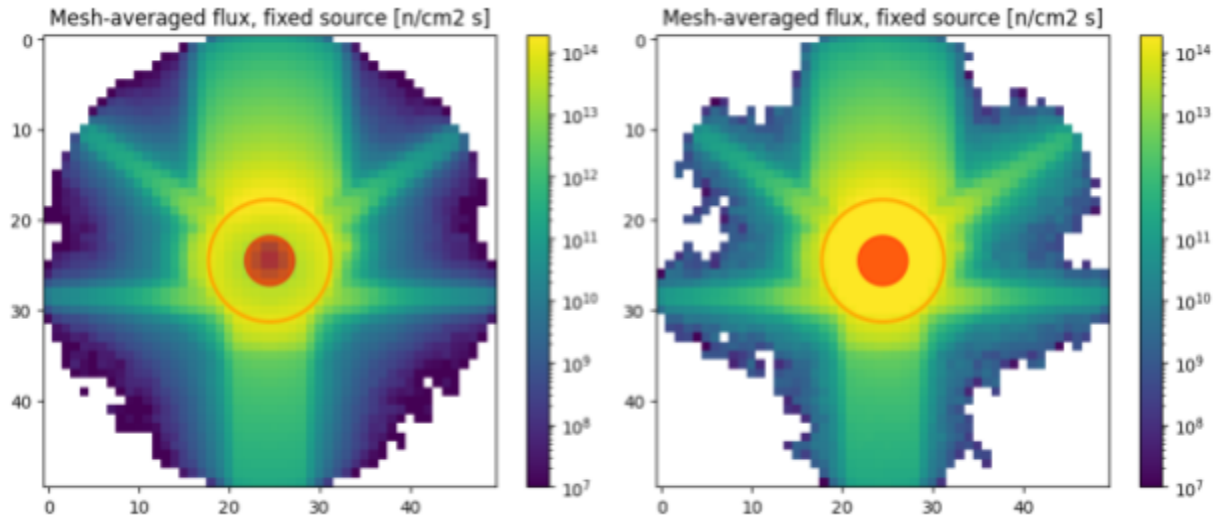

Figure 3: 2D plot of statistical error in dose at the z=0 midline of the MK2 TRIGA reactor. Left: surface source, 18864.13s runtime. Right: eigenvalue, 3300s.

2.3 Shannon Entropy

In this work, two candidate methods of quantifying the stationarity of a surface source were developed and evaluated: tracking the batch-by-batch convergence of particle trajectory spatial density and energy together via multidimensional Shannon entropy[4], as well as a means of more finely quantifying the convergence of particle energy distribution in space by tracking the convergence of spatially-dependent effective reaction rates with various materials.

The first method of quantifying the convergence of the spatial density of particles evaluated was tracking the stabilization of the Shannon entropy[4] of the spatial distribution of neutrons incident on a mesh drawn over the surface for banking particles.

Currently, Shannon entropy is used in Monte Carlo transport codes to determine when a simulated fission source has reached stationarity. OpenMC, like other transport codes, relies on a power iteration technique to solve k-eigenvalue problems. As the initial fission source is not known prior to beginning the simulation, an initial source (often a point source at the center of the fissionable material) is defined, and then iterated upon each generation until it reaches stationarity. Because of this, k-eigenvalue problems are solved in two stages: inactive batches, where the fission source reaches stationarity, and active batches, where tallies are tracked and contribute to the ultimate measures of k_{eff}, reaction rates, and flux/dose maps produced by the simulation. It is critical to accurately know when the fission source reaches stationarity and active batches can be triggered, as counting tallies prior to converging the fission source will introduce significant bias into the results. Conversely, triggering the active batches long after the source has reached stationarity will unnecessarily extend computational time.

Evaluating stationarity of the fission source is difficult, as even when converged significant statistical noise is still present. It was originally thought that the convergence of generation-wise values of k_{eff} itself was a sufficient measure of fission source convergence, but it was later understood that k_{eff} converges before the fission source[4]. Since that acknowledgement, Shannon entropy has been a widely-accepted metric in evaluating fission source stationarity[7]. Shannon entropy is used to evaluate fission source convergence by quantifying the spatial distribution of fission source sites over a 3D mesh drawn over the active core as a scalar value. Once this scalar value has reached stationarity within some statistical bounds, the fission source is said to be converged.

Likewise, the mesh used in this work divides the cylindrical banking surface into a predetermined number of bins in both the θ and z directions as they are defined in a reactor's OpenMC geometry. However, now the particles in each bin represent particles banked on the surface source in the physical region enclosed by the bin, rather than the location of a fission site. The convergence of the fraction of total particles binned in each θ, z bin, and thus the overall spatial distribution of particles banked on the surface, is quantified by the convergence of a single value: the two-dimensional Shannon entropy of the distribution, where is $p(x_{z,\theta})$ is the fraction of particles banked in a particular mesh cell, re-calculated and tracked as each successive batch of new particles was banked in the source:

Equation 1. $$S(X) = -\sum_{z}\sum_{\theta} p\left(x_{z,\theta}\right)\log_2 p\left(x_{z,\theta}\right)$$

Unlike previous work with Shannon entropy that concerned only the physical distribution of fission sites, Shannon entropy was used in this work to also simultaneously evaluate the convergence of particle energy distribution within three bins representing thermal, epithermal, and fast neutrons. Energy was represented as another dimension of bins, and Shannon entropy was calculated similarly:

Equation 2. $$S(X) = -\sum_{z}\sum_{\theta}\sum_{E} p\left(x_{z,\theta,E}\right)\log_2 p\left(x_{z,\theta,E}\right)$$

In this work, particle trajectory was considered via two use case-dependent means. When the distribution of particles banked on the entire cylindrical surface surrounding the core was considered, banked particles were filtered by calculating the dot product of individual trajectories with the normal vector to the surface and only storing particles that were traveling away from the core. In cases where higher fidelity was necessary, such as simulating the particle flux within and adjacent to the model reactor's narrow, air-filled beam ports, **Eq. 2** was modified to include bins representing the azimuthal and polar components of particle trajectories in the place of energy, the convergence of which was evaluated separately.

2.4 Legendre Polynomials

The second method used was tracking the convergence of particle energy distribution in space via the continuous calculation of the coefficients of functional polynomial expansions associated with spatially-dependent "effective reaction rates" of the particles in each bin with a set of different Z materials.

Functional expansions, such as Fourier series, enable the expression of a function via the infinite sum of a set of coefficients multiplied by an orthogonal basis set. By looking at the batch-by-batch convergence of the lower-order coefficients necessary to reconstruct the function, the stationarity of the complex shape of the function can be deduced, rather than just its average. For this application, Legendre polynomials (**Fig. 4**) were chosen as the orthogonal basis set, and the functions to be considered were the spatially-dependent effective reaction rates of the particles banked on the surface source. Legendre polynomials were selected due to their simplicity and ability to demonstrate the stability of necessary higher-order moments of spatially-dependent effective reaction rates.

As a note, Legendre polynomials are only orthogonal in flat dimensions—in this case, the z direction on the surface source. For the test problem used in this work, the neutron flux was nearly uniform in theta, therefore the most conservative determination of stationarity would come from analysis of spatial dependence in z. For problems in which spatial dependence in other dimensions is more complex, the same procedures detailed in this work could be used with any basis set.

Using effective reaction rates allows for a more complete and useful quantification of energy distribution of particles—an effective reaction rate provides a single-value measure of the entire neutron or photon energy spectrum within each spatial bin, and provides a physically-useful predictive measure of dose and potential shielding effectiveness. This quantification by measuring the stationarity of the first 6 coefficients of Legendre polynomial basis set associated with total neutron reaction rates as a function of particle location on the cylindrical surface source (θ, z).

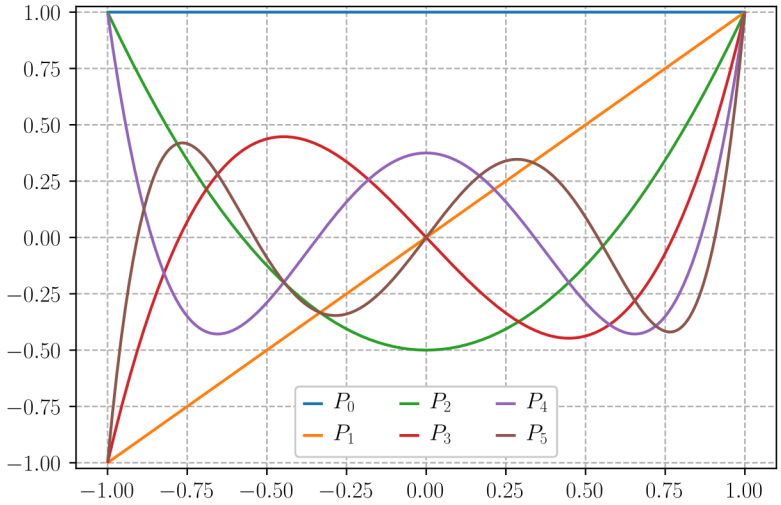

Figure 4. The first six Legendre polynomials

2.5 Determination of stationarity criteria

To develop both the Shannon entropy and functional expansion means of determining banked source stationarity, a robust test case is necessary. The parameters of both methods require tuning to demonstrate source stationarity separable from noise, and prior to this work, it was not known how many particles or batches needed to be simulated such that enough particles were banked to demonstrate surface source stationarity at various resolutions in space and energy.

A test case that accounts for these unknowns necessitates a particle and batch count high enough that enough particles are banked to demonstrate surface source stationarity at different resolutions. To provide an adequate basis for determining the effectiveness of surface source banking as a methodology, an OpenMC reactor model that includes far-field regions of the geometry was chosen. As particles were banked on the surface source at each batch, the stabilization of the 2D spatial Shannon entropy was tracked, as well as the Legendre polynomial coefficients describing spatially-dependent total neutron reaction rates over the mesh. From the analysis of this data, a set of recommendations for concrete convergence conditions was determined.

Together, these tolerances (convergence criteria), the mathematical and computational framework used to establish them, and the implementation and evaluation of these methodologies in OpenMC are the final outputs of this thesis work. The analysis carried out during this process evaluates the potential of each methodology to accelerate and refine the far-field flux simulations of relevance to the design of advanced nuclear systems, with the intent of extending the applicability of OpenMC towards industry-standard work in high-fidelity shielding design.

3. Methods

3.1 Reactor model (test case) overview

An existing, validated OpenMC model of the Mark II TRIGA (Training, Research, Isotopes, General Atomics) reactor housed at the Institute Jožef Stefan[9] was used for the entirety of this thesis work. This model includes the active core as well as the extensive concrete, water, and long graphite thermalization columns extending off the core region. The presence of these regions is necessary for validating the potential of surface-source-banking methods to accelerate far-field flux and dose simulations. While not present in the core model plot shown in Figure 6, all of the air-filled beamports have been included in the model geometry. The reactor facility is shown below in **Fig. 5**, and the core diagram and OpenMC model in **Fig. 6**.

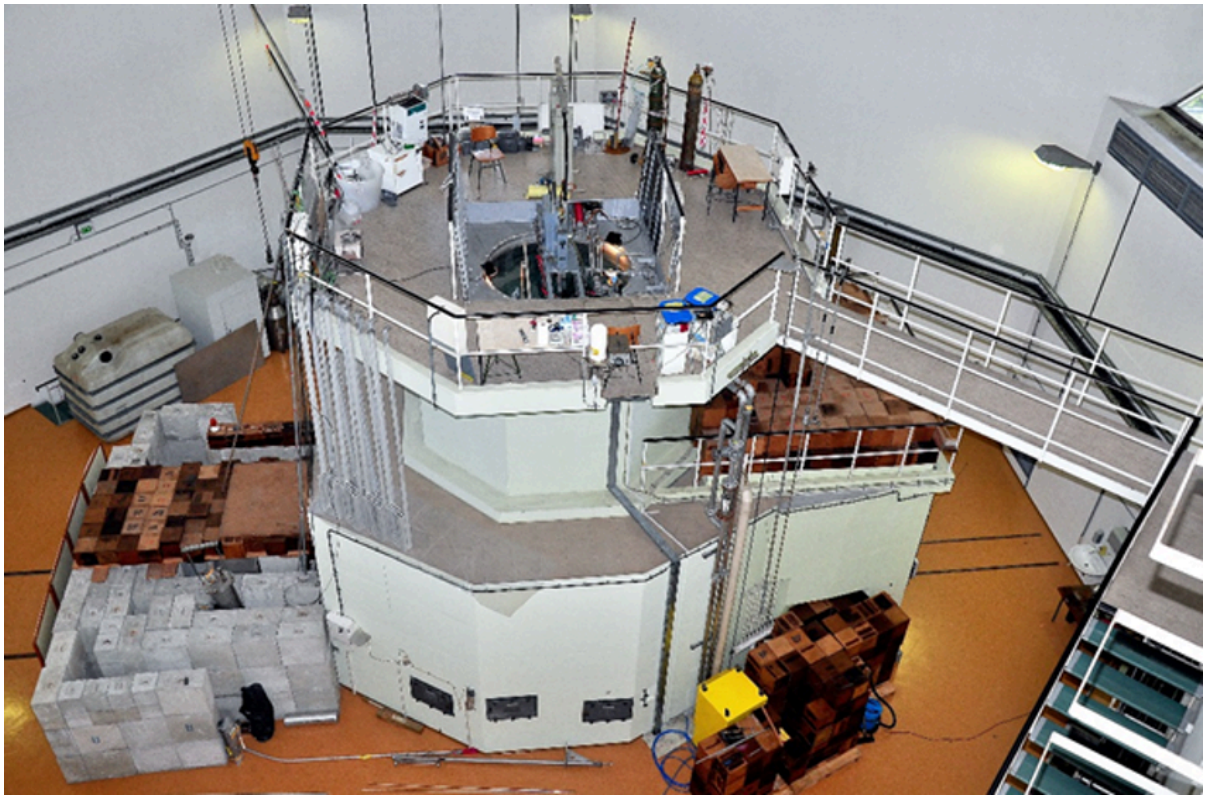

Figure 5. IJS MK2 TRIGA facility[9]

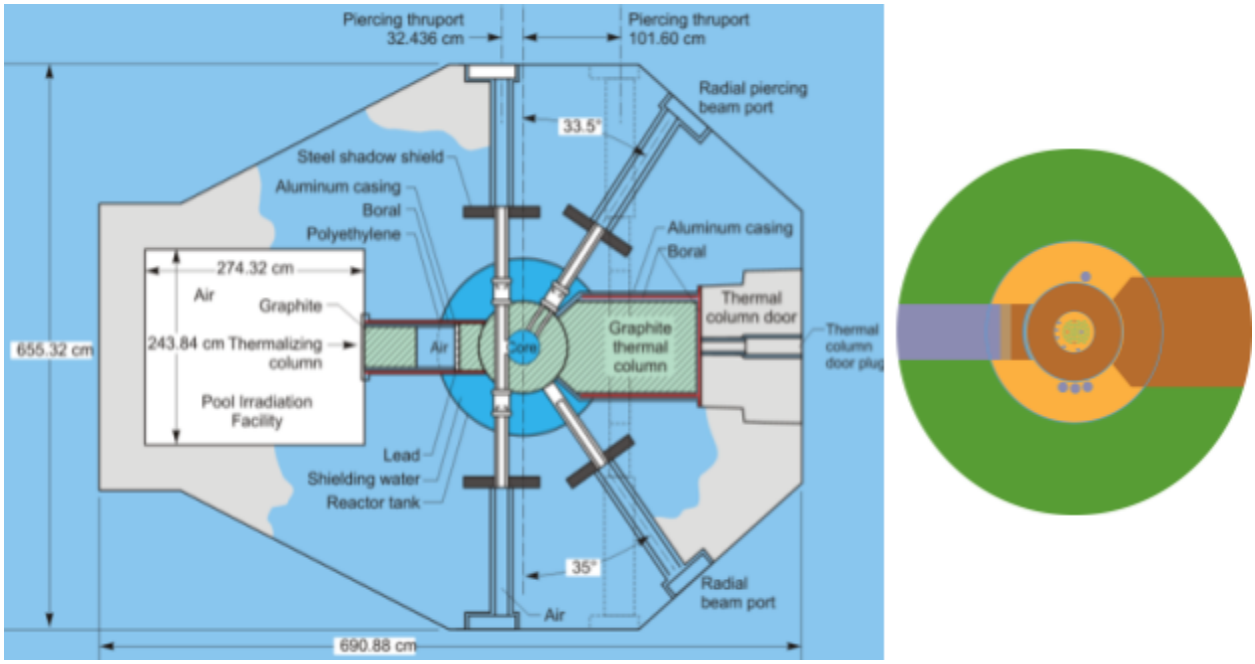

Figure 6. 2D reactor diagram[9] and 2D slice of the OpenMC core model

3.2 Modifications to OpenMC source

For all OpenMC cases run for this work, the OpenMC source code for the most recent release (15.0) was modified to enable more robust, batch-dependent analysis of banked particles, and to avoid banking the same particle multiple times. Rather than creating a single surface source bank, or generating surface source files on an as-needed basis when a pre-set maximum number of particles is banked, one surface source file is generated with all particles that cross it on a batch-by-batch basis, allowing batch-by-batch post-processing and analysis of the surface source particles.

Additionally, the source code for particle definition and source banking was modified to improve the source-banking functionality itself: at present, OpenMC banks every surface crossing as an individual particle, resulting in the same particle being represented by an average of 2.5 separate particles in the source bank on the selected surface of this problem. This is most likely an oversight in the OpenMC source that will be reported at the conclusion of this work. Typically, surface sources are spatially much further from the core, where this effect is minimal and has thus gone undetected until now. Unaltered, this results in over-representation of thermal neutrons in the surface source, and clustering effects that can be seen in stationarity analysis of the source. To resolve this, unique particle IDs are now stored along with other particle attributes when particles are banked, allowing duplicates to be filtered out during post-processing of source files. The significance of this effect on the banked particle energy spectrum, and results of utilizing a surface source in fixed source mode are shown in **Sec. 5.2**.

3.3 Fission source stationarity

Shannon entropy, as discussed in the previous section, was initially used in its traditional context to evaluate the stationarity of the distribution of fission sites during the inactive batches of the simulation. As shown in **Fig. 7** below, the convergence of the fission source distribution was confirmed to occur during batch 17. Fission site distributions were evaluated each batch based on their location within a coarse (8x8x8) mesh. The stationarity criteria used[7] deems fission site stationarity reached when the sample means of the Shannon entropy calculated within a specified window stabilize within a predetermined statistical tolerance.

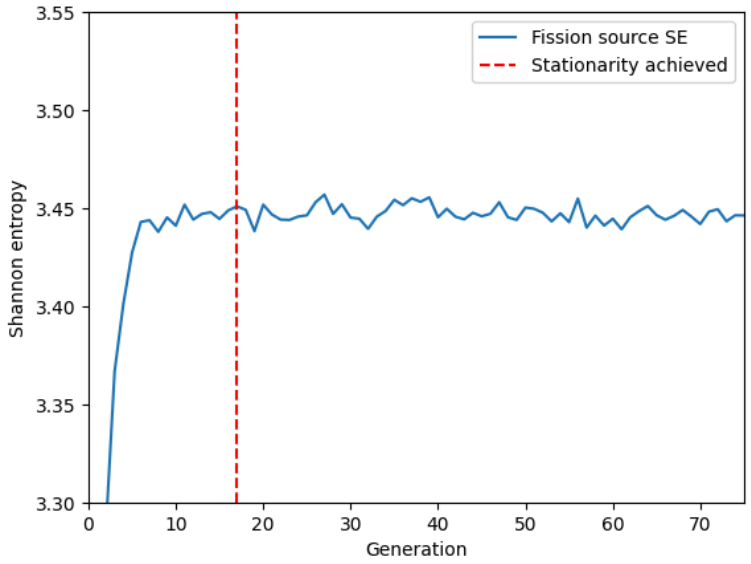

Figure 7. Shannon entropy of the fission site distribution

This confirmation was essential to establish prior to running a much longer eigenvalue case to bank a surface source around the core, as an inaccurate internal distribution of fission sites would result in an inaccurate spatial distribution of particles banked on the surface source just outside the region. With this in mind, only particles banked in batches after fission source stationarity was reached during the 17th batch are considered in this analysis and included in the final accumulated surface source.

3.4 Eigenvalue case setup

A high particle count eigenvalue case that simulates the entire reactor geometry is necessary to both bank particles to create surface source files with and generate high-fidelity baseline neutron dose and flux maps to compare the results of later (fixed) surface source-based simulations to. The first case was run over 750 batches, with 1E+6 particles per batch. The high particle and batch count was utilized to ensure that enough particles would be banked such that the convergence points of relevant variables and distributions could be observed at fine

resolutions within position, energy, or trajectory space.

This eigenvalue case was set up with track length estimator tallies to record neutron dose and flux over a 3D mesh spanning the entire reactor geometry, as well as the neutron current passing through the surface source mesh. The results of this case served to establish a baseline set of results to compare fixed source simulations utilizing the surface source to.

3.5 Eigenvalue - fixed source equivalence

Additionally, a current tally through the surface source mesh recorded in the eigenvalue case was used to equate dose and flux between the eigenvalue case and fixed source cases. In OpenMC, tallies are normalized in terms of the number of source particles simulated, and recorded in units of [units/source], rather than in physical units. Instead of the flux in the eigenvalue case being returned in [particles/cm2-s], it would be reported in units of [particle-cm/source]. To convert OpenMC's result for neutron flux within a given mesh cell to something more intuitive, one must scale via the anticipated thermal power of the reactor. This is accomplished by tallying a heating score, *H'* over the entire system and performing unit conversion such that it is in [J/source]. As shown below in **Eq. 3**, the anticipated reactor power *P* in [J/s] can be divided by the heating score to give a scaling factor *f*, in [source/s] that can be used for other all tallies[8]. In this case, in accordance with the standard steady-state operating power of the TRIGA MK2 reactor, *P*, was set to 50 kW:

$$\textbf{Equation 3.}\quad f = \frac{P}{H'} = \frac{[\mathrm{J/s}]}{[\mathrm{J/\ source\ }]} = \left[\frac{\mathrm{source}}{\mathrm{s}}\right]$$

This scaling factor can then be used to convert tallies into physical units. An example of this is the conversion of OpenMC-reported flux ϕ, in [particle-cm/source], to ϕ' [particles/cm2-s]. **Eq. 4** demonstrates this conversion, where *V* is the mesh cell volume, which is uniformly 1,280 cm^3 for all cases simulated in this work since we are using a uniform mesh tally.

$$\textbf{Equation 4.}\quad \phi' = \frac{f \cdot \phi}{V} = \frac{[\ \mathrm{source}\ /\mathrm{s}] \cdot [\ \mathrm{particle\text{-}\ cm/\ source}\ ]}{[\mathrm{cm}^3]} = \left[\frac{\mathrm{particle}}{\mathrm{cm}^2 \cdot \mathrm{s}}\right]$$

However, this conversion is less straightforward for the fixed source case, as fixed source cases cannot utilize global heating tallies to establish conversion factors between reactor power and tally counts. This equivalence is still necessary for comparing accuracy between the two methods and generating physically-useful results from fixed source cases. First, a global heating tally and subsequent score is used according to **Eq. 4** in the eigenvalue case to find the neutron flux as averaged in each 8x8x20 cm mesh cell in the reactor geometry, $\phi'_{eigenvalue}$ in [particles/cm2-s].

The effective source strength from the eigenvalue case, or *f*, in [source/s] required to find

$\phi'_{eigenvalue}$ cannot then be directly used as the source strength in the fixed source case: the majority of source particles simulated in the eigenvalue case are either absorbed or reflected back into the core prior to crossing and being banked on the surface source. The ratio of banked particles to eigenvalue source particles is analogous to the total current tallied passing through the surface source mesh in the positive direction, ${}^{+}J_{eigenvalue}$, as it is recorded directly by OpenMC in [surface crossings/source]. As particles that pass through the surface source mesh are often double-counted in the current tally ${}^{+}J_{eigenvalue}$, an additional correction factor is needed to account for the surface source not containing these duplicates. Considering both these factors, **Eq. 5** shows an expression for a corrected ϕ'_{fixed} in [particles/cm2-s]. Given a well-defined surface source bank and a substantial number of particles simulated in both the eigenvalue and fixed source cases, ϕ'_{fixed} and $\phi'_{eigenvalue}$ should be equivalent.

Equation 5.
$$\left(\frac{\phi \cdot f}{V}\right) \cdot J^{+}_{\text{eigenvalue}} \cdot \left(\frac{n_{\text{total}} - n_{\text{repeats}}}{n_{\text{total}}}\right) = \phi'_{\text{fixed}} \sim \phi'_{\text{eigenvalue}}$$

3.6 Source banking mesh

The mesh for particle banking, or tallying current through the mesh for the 750 batch eigenvalue case, was placed centered around the core center at x,y = 0,0, with a radius of 54 cm corresponding to the boundary of the active core region. The mesh covers all z of the reactor model, from the top vacuum boundary to the bottom vacuum boundary. This mesh, divided into bins similar to that which will be used for stationarity analysis of the particles banked on it, is shown below in **Fig. 8**.

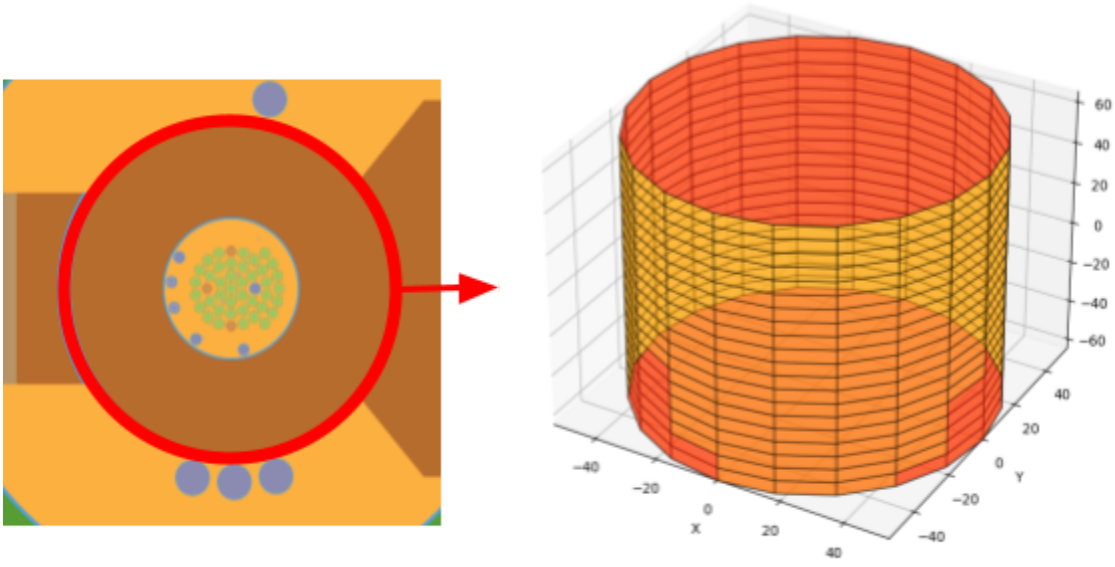

Figure 8. Active core geometry as simulated in OpenMC, and surface source mesh

4. Stationarity criteria development

4.1 Shannon entropy evaluation of spatial particle distribution on the surface source

After running the 750 batch eigenvalue case and generating a unique source particle file for all neutrons that passed through and were banked on the surface source during each active batch, it was possible to begin post-processing the files to develop a set of stationarity criteria. It was anticipated that relevant features—spatial distribution of particle energy and flux density—would reach stationarity long before the 750th batch of particles was added to the cumulative surface source file, but this allowed for investigating smaller features of the neutron energy spectrum and finer spatial resolution if desired.

From a physical perspective, spatial bin sizes were chosen to capture relevant features of the geometry at a resolution fine enough to reflect the NRC CFR 36.25 regulation[6] on shielding: *dose measurements may not be averaged over an area greater than 20 cm in any linear dimension*. Dividing the surface source mesh into 20 bins in the z direction and 20 in the θ direction resulted in spatial bins with an arc length of 17 cm and height of 7 cm. The bins in the *z* dimension are sized via adaptive binning to avoid extremely low population bins in low flux regions and skewing the entropy result, and the θ bins are equally spaced between 0 and 2π. The relative flux density and number of neutrons "stored" in each spatial bin is plotted in **Fig. 9.**

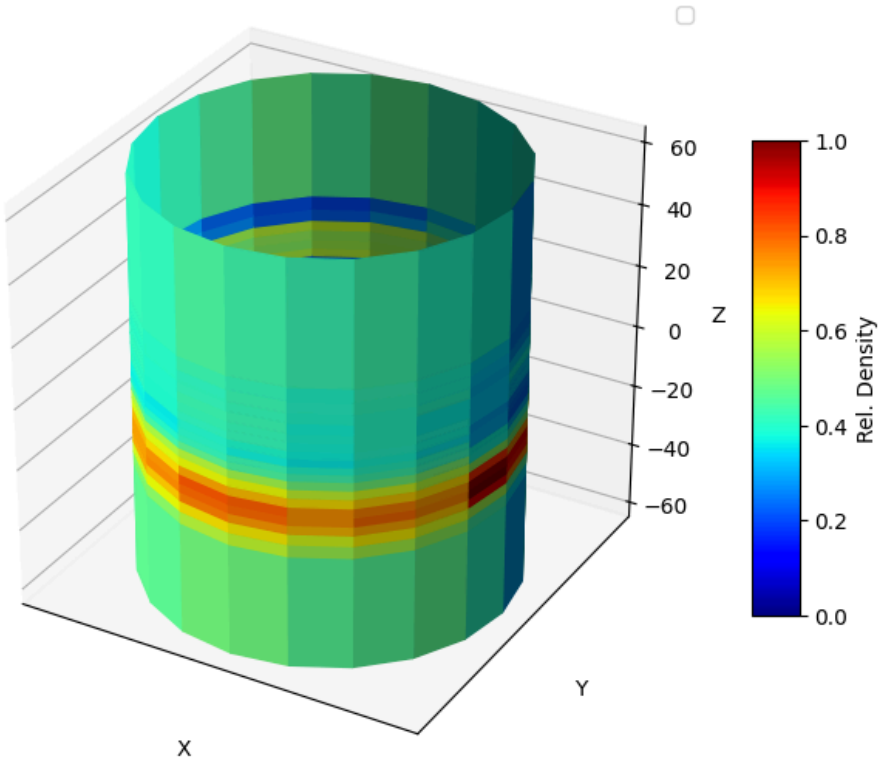

Figure 9. Banked neutron density through each spatial bin on the surface source

From a statistical perspective, bin size determination is crucial to achieving useful stationarity results with Shannon entropy. Shannon entropy reflects the stabilization of the fraction of all particles residing in a certain bin (describing a region of spatial and energy space), and for the purposes of this paper is continuously re-evaluated as more particles are added to a cumulative surface source, batch-by-batch. Up to a certain threshold, more bins in a given dimension allows the stationarity of particle distributions in that dimension to be evaluated on a finer scale.

However, the nature of Shannon entropy presents a limitation with this assumption. Consider again **Eq. 1**, the expression for Shannon entropy. If enough bins are used such that initially no particles accumulate in certain bins, the contribution of those bins to the evaluated Shannon entropy is zero, artificially lowering its value. This effect would be more severe in the first few batches where Shannon entropy is calculated, and gradually improve as more particles accumulate in the bins. Given an extremely large number of bins relative to the number of particles banked each batch, the numerical convergence of Shannon entropy would be reflective of the eventual filling in of empty or very low population bins rather than the stationarity of the particle flux itself.

Additionally, the value of Shannon entropy itself and the relative size of its fluctuations are bin size-dependent. More bins results in a larger Shannon entropy value, and smaller batch-by-batch fluctuations relative to that value. When many bins are utilized, these effects together make the evaluation of stationarity challenging: running means must be evaluated over a large window size to capture the cessation of gradual trends in Shannon entropy rather than shorter-term fluctuations.

To demonstrate these effects and identify a suitable bin configuration for this use case, Shannon entropy of source particles was evaluated cumulatively for the spatial and energy distributions of neutrons banked on the surface source for several different bin configurations. It should be noted that evaluating the convergence of the multi-dimensional Shannon entropy associated with the surface source on a batch-by-batch basis, rather than cumulatively, does not demonstrate stationarity, only statistical noise. This effect is shown in **Fig. 10**, where both batch-by-batch and accumulated Shannon entropy are plotted together for the 20 z, 20 θ, and 3 energy bin configuration.

As true for any reasonable bin configuration, each batch is a true random representation of the source, and accumulation of particles between batches is necessary to accurately characterize the flux through the surface source mesh. The accumulated Shannon entropy is higher than the average of the individual batches, since it eliminates the number of empty bins that naturally occur from the random filling of the surface source. The accumulated Shannon entropy thus provides an indication that the full space is represented.

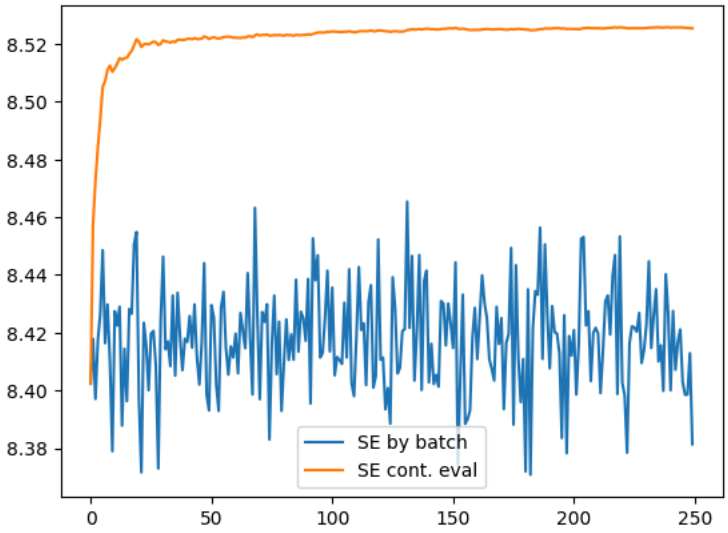

Figure 10. Batch-by batch (blue) and accumulated evaluations of Shannon entropy

To comparatively examine the effects of finer bin configurations, the same particles were then divided spatially into bins delimiting 20, 40, and then 100 regions per spatial dimension. Three bins were used to roughly characterize the energy distribution of the particles in both cases. The fast neutron range is capped at the maximum energy of the ENDF/B-VII.1 nuclear data library used for the simulations in this work, at 20 MeV.

Table 1. Neutron Energy Bin Edges

Thermal	Epithermal	Fast
0 - 0.68 eV	0.68 - 1e6 eV	1e6 - 20e6 eV

The same stationarity metric was used to provide a quantitative measure of when enough surface source particles had accumulated such that the source could be considered to have stabilized in space and energy for all three cases. The metric used previously for fission site stationarity is not applicable to this case, where accumulated rather than instantaneous properties of the dataset are considered and statistical noise inherently decreases between batches. This metric considers stationarity to be achieved when relative differences between consecutive values of the Shannon entropy running mean remain below a set threshold over a given window. The window size was set to twenty-five batches, and the threshold set to 2.5×10^{-6}: stationarity was said to be achieved when the running mean changed less than the threshold value between windows. The accumulated Shannon entropy for each case with vertical lines indicating stationarity according to this metric is shown in **Fig. 11**.

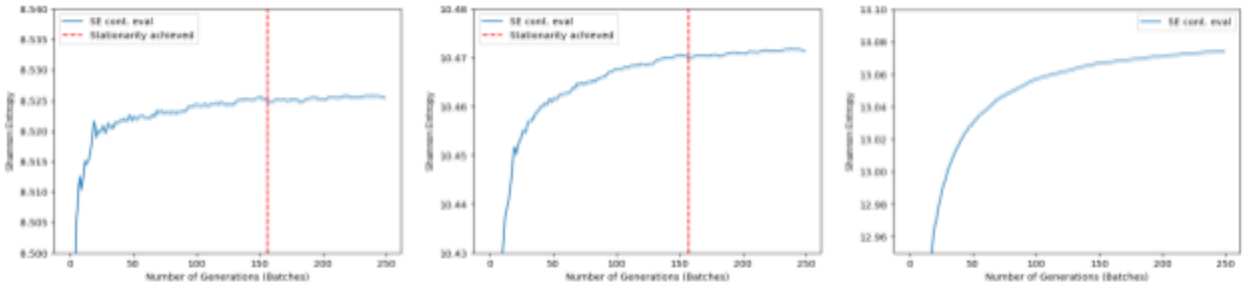

Figure 11. From left to right: 20 bins per spatial dimension, 40, and 100

In the 20 and 40 bins per spatial dimension case, the stationarity was achieved via the above metric at, respectively, 156 and 157 batches. It was not achieved within the shown window in the 100 bins per spatial dimension case. This is an interesting result: while the 40 bin case shows some "rounding" from empty bins artificially lowering the Shannon entropy value in early batches, enough particles eventually accumulate in these bins such that this effect is resolved early enough such that stationarity is indicated at roughly the same batch number as the 20 bin case. For the 100 bin case, with 25x the total bins of the 20 bin case, this effect takes much longer to resolve, stationarity is not achieved until after the 450th batch. While "stationarity" is eventually achieved numerically, it is more representative of the gradual filling in of very low-population bins and not a useful means of determining convergence of the flux incident on the banking surface: with $3x10^4$ bins total in the highest bin-count case, and roughly $4.7x10^3$ particles accumulated per batch, significant negative skewing of Shannon entropy is to be expected even as particles up to those simulated in later batches are accumulated.

The reduction of relative fluctuations and increase in the value of Shannon entropy with higher bin counts is also apparent: at the scale shown, almost no noise can be seen in the 100 bin case.

The 20 z, 20 θ, and 3 energy bin configuration both aligns with the NRC CFR 36.25 requirement, and avoids the challenges associated with low-population or empty bins more clearly than the 40 bin per spatial dimension case. With this bin configuration and the previously defined stationarity metric, the surface source achieved stationarity in space and a coarse measure of energy after all particles banked up to the 156th active batch were added to the source, as shown below in **Fig. 12.**

It will be shown in **Sec. 5** that using this criterion as a means of establishing source stationarity and definition is effective in ensuring that the banked particles can accurately serve as a proxy for the fissioning core for cases that concern larger spatial regions of interest, and lack void regions with narrow geometry.

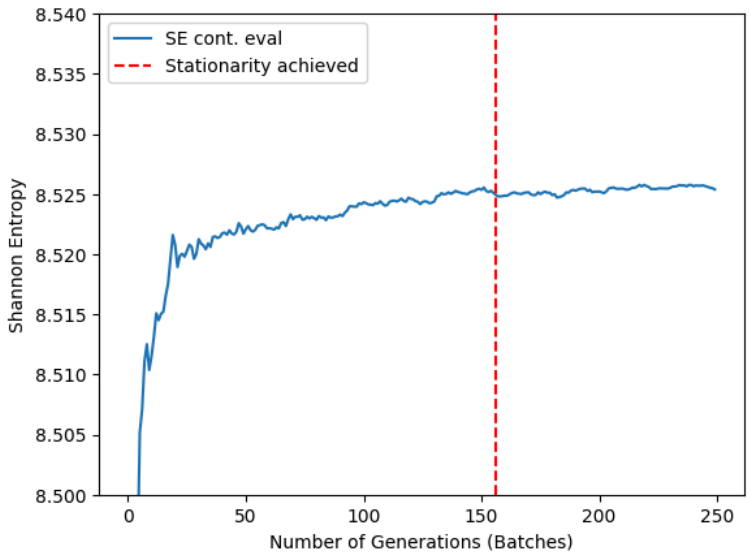

Figure 12. Stationarity evaluation, 3D Shannon entropy

However, one thing that this 3D Shannon entropy approach leaves to be desired is a finer, more physically-attuned approach towards quantifying the spatially-dependent neutron energy distribution. While three energy bins captures this coarsely, fine features of the energy spectrum in the presence of higher-Z materials can significantly affect reaction rates through resonances. For this reason, the same 3D Shannon entropy approach was attempted with 20 logarithmically spaced energy bins, and 20 per spatial dimension, for a total of 8000 bins. The result is shown below in **Fig. 13**.

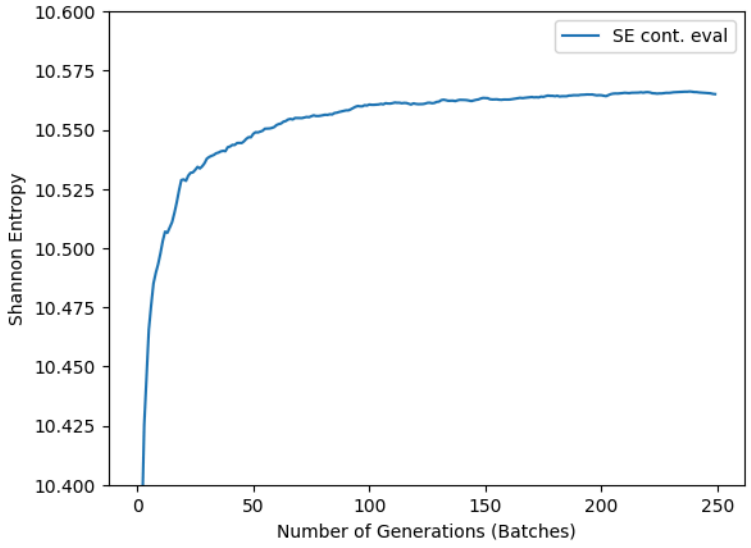

Figure 13. 3D Shannon entropy evaluation, 20 energy bins

Like the 100 bins per spatial dimension case, the impact of zero or very low particle bins in early batches is significant enough that Shannon entropy stationarity is not achieved within 250 batches. Again, rather than showing that it takes the accumulation of particles through more batches to more finely define the energy distribution, the numerical convergence of Shannon entropy here would demonstrate that enough particles have been banked such that previously empty or low-population bins have been filled. However, the reaction rate-based means of evaluating surface source stationarity is a promising means of overcoming this limitation.

4.2 Reaction rate-based methodology for finer energy spectrum stationarity analysis

As discussed briefly in the previous section, for the purposes of shielding design and dose calculations, accurately defining the spatially-dependent neutron (or photon) energy spectrum banked on a surface source is critical. The three energy groups included in the multi-dimensional Shannon entropy approach previously reviewed offer some insight into the energy spectrum, but neglect finer, but important features like resonances. To overcome this limitation, a means of confirming the energy distribution of the banked particles based on spatially-dependent effective cross section with different Z materials was evaluated.

For this application, an "effective cross section" is analogous to a one group total cross section calculated with all of the neutrons in a spatial bin. **Eq. 6** provides the standard expression for an effective single group cross section, where ϕ(E) is energy-dependent surface flux of outgoing particles from the source bank, σ(E) the energy-dependent total cross section:

$$\textbf{Equation 6.}\quad \sigma_g = \frac{\int_0^\infty \sigma(E)\,\phi(E)\,dE}{\int_0^\infty \phi(E)\,dE}$$

Finding this effective cross section enables quantification of the entire energy spectrum through a single value, as the calculation involves integrating the energy-dependent total cross section over the energies of all particles of interest, capturing finer features of the energy spectrum through the cross section's complex energy-dependence. Applied discretely to the neutrons banked within a specific spatial bin, the effective reaction rate within a bin takes on the form in **Eq. 7,** where N_{bin} is the total number of neutrons banked in the bin:

$$\textbf{Equation 7.}\quad R_{\text{eff}}(\ \text{bin}\ ) = \frac{\sum_{i\in\text{bin}} \sigma\,(E_i)}{N_{\text{bin}}}$$

Within one bin, for example, the 10th z bin and 10th theta bin, the effective cross section of neutrons banked on the surface source with H_2O can be tracked as more particles are added to the bin each batch:

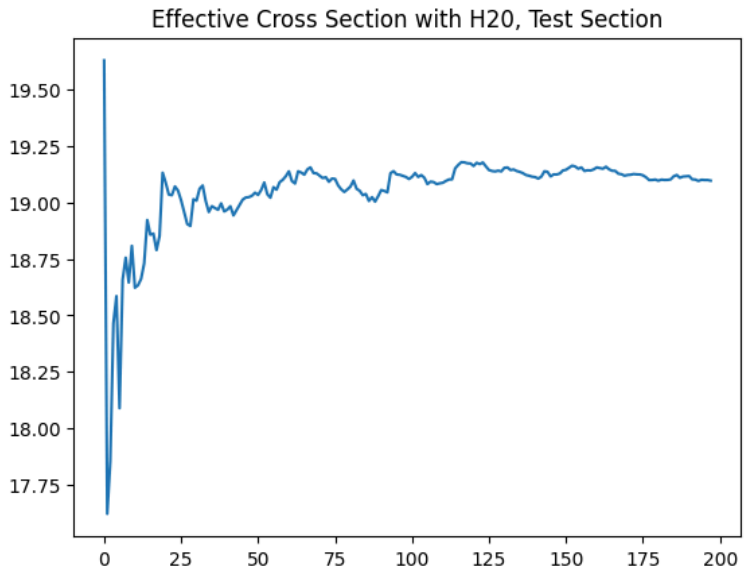

Figure 14. Effective cross section (b) of H2O with neutrons banked in one spatial bin

Even with a relatively low-Z material where resonances do not significantly influence reaction rates, the effective reaction rate in the single spatial bin does not appear to converge until around the 150th batch of neutrons are banked. For a true measure of the energy distribution, the effects of space and resonances of higher Z materials will need to be considered. As the core is not infinite in the z direction and has some non-uniformity in the theta direction, the neutron energy spectrum will not be uniform throughout the surface source—some means of quantifying its variation in space is required.

Orthogonal basis sets provide a means of capturing the convergence of effective reaction rates and their spatial dependence, and by extension, determining when the stationarity of the neutron energy spectrum and its spatial variations has been achieved for a banked surface source. Legendre polynomials, as shown in **Fig. 4**, form an orthogonal basis set and can be used to reconstruct other spatially-dependent functions in a single dimension. When the stabilization of the coefficients used to reconstruct a function with Legendre polynomials is achieved, stationary of that function in space has been reached.

Legendre polynomials take on the following general form, where $P_n(x)$ is the nth degree Legendre polynomial:

Equation 8. $$P_n(x) = \frac{1}{2^n n!}\frac{d^n}{dx^n}\left[\left(x^2-1\right)^n\right]$$

Functions can be represented as a summation of Legendre polynomials by normalizing their domain to [-1, 1], and finding all coefficients c_n such that the normalized function $f(x)$ can be reconstructed as follows:

Equation 9. $f(x) = \sum_{n=0}^{\infty} c_n P_n(x)$

The effective cross section described in **Eq. 7** as a function of the spatial dimension z can be reconstructed with the first six Legendre polynomials by calculating the associated coefficients c_n for $n \in \{0,1,\ldots,6\}$ at a given batch. These coefficients are calculated by passing in the bin-wise effective cross sections to the NumPy polynomial.legendre module. **Fig. 15** demonstrates Legendre polynomial reconstruction of the effective total cross section of neutrons with ^{184}W as a function of *z* after the first 200 batches of neutrons have been accumulated in the surface source.

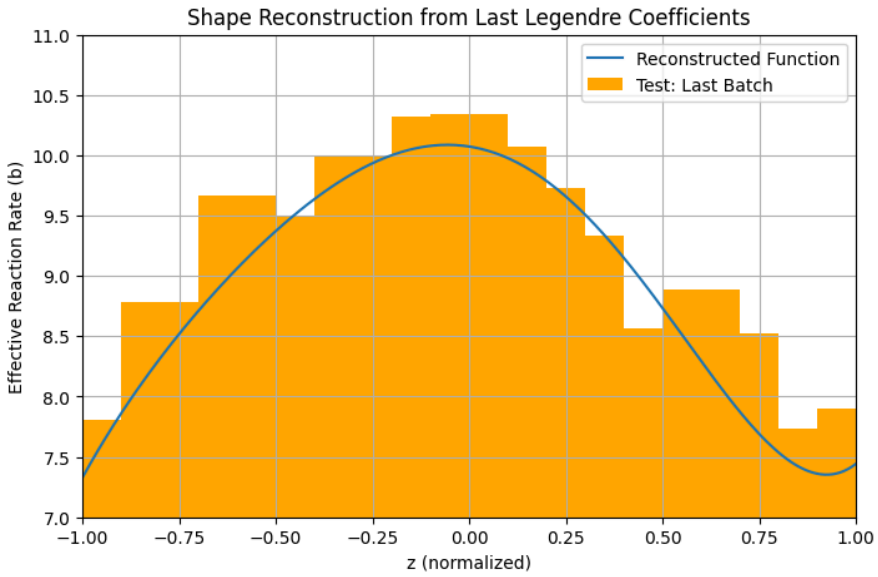

Figure 15. Legendre polynomial reconstruction of ^{184}W effective xs at batch 200

Stationarity of an effective cross section as neutrons accumulate in the spatial bins each batch can be established via the stationarity of the Legendre coefficients c_n used to reconstruct the effective cross section's spatial dependence. For this use case, only the *z*-dependence of effective reaction rates was considered, as the MK2 TRIGA core geometry is effectively azimuthally uniform. As mentioned in **Sec 2.4**, should θ-dependence be considered, the domain would either need to be converted to $\cos(\theta)$, or another orthogonal basis set utilized. To cover a range of different Z materials, ^{184}W, H_2O, and ^{12}C were considered. Their total energy-dependent neutron cross sections as reported in the ENDF/B-VII.1 nuclear data file, are shown below in **Figure 16**.

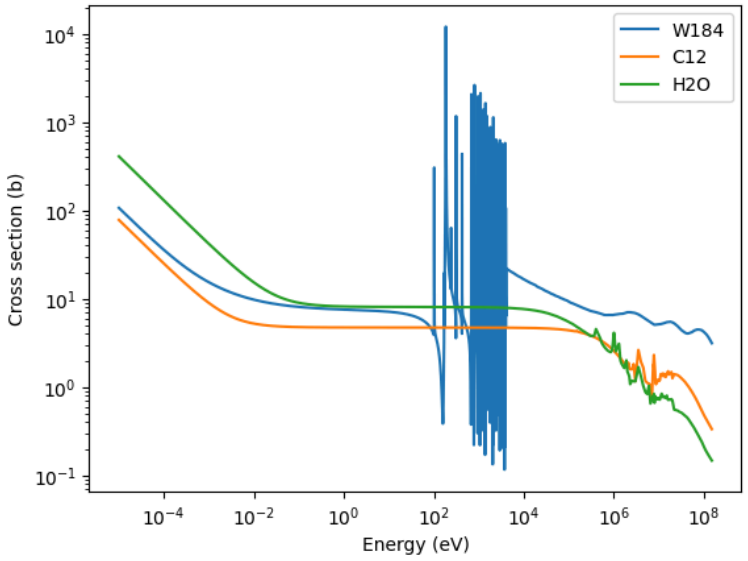

Figure 16. Total neutron cross sections of materials considered

Legendre coefficients for the effective cross sections of each of these materials and their z spatial dependence were evaluated as neutrons accumulated in the spatial bins each bach. These coefficients are plotted in **Fig. 17-19** below. Convergence, or stationarity of a coefficient was considered achieved when the absolute change in its running mean remained below 1% for 25 consecutive batches.

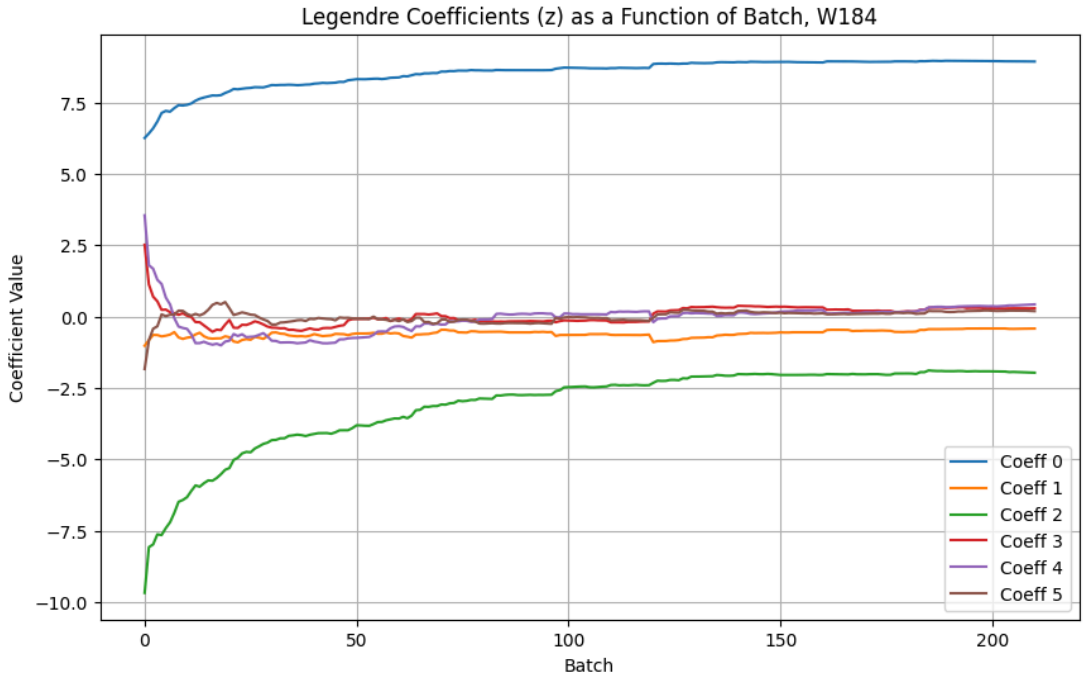

Figure 17. First six Legendre coefficients for ^{184}W effective cross section as a function of z

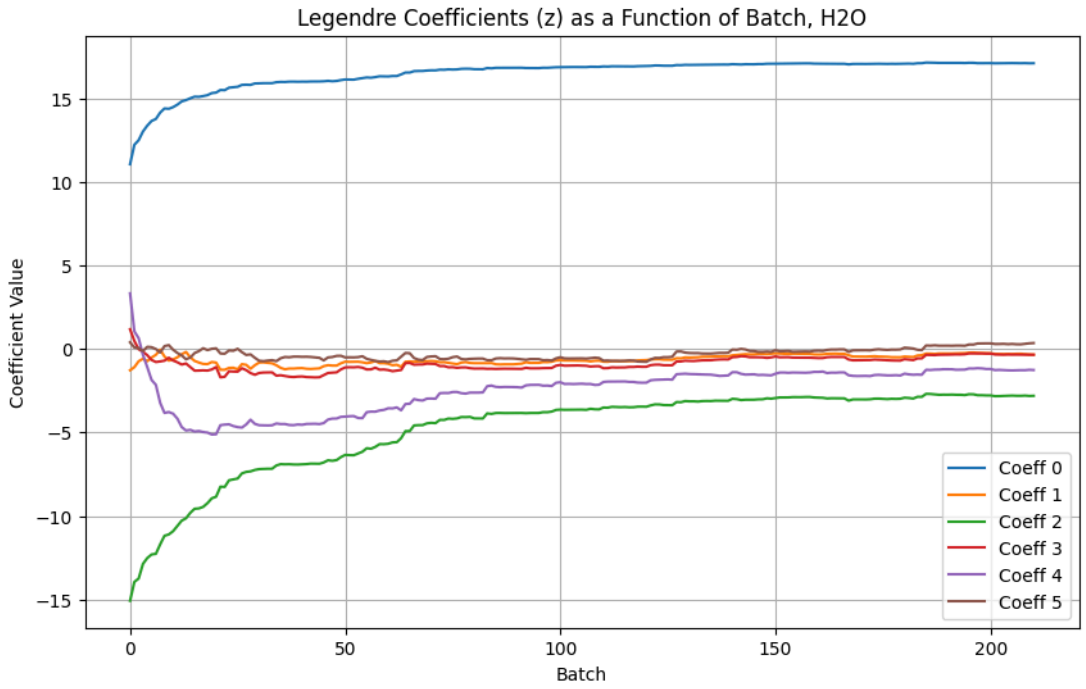

Figure 18. First six Legendre coefficients for H_2O effective cross section as a function of z

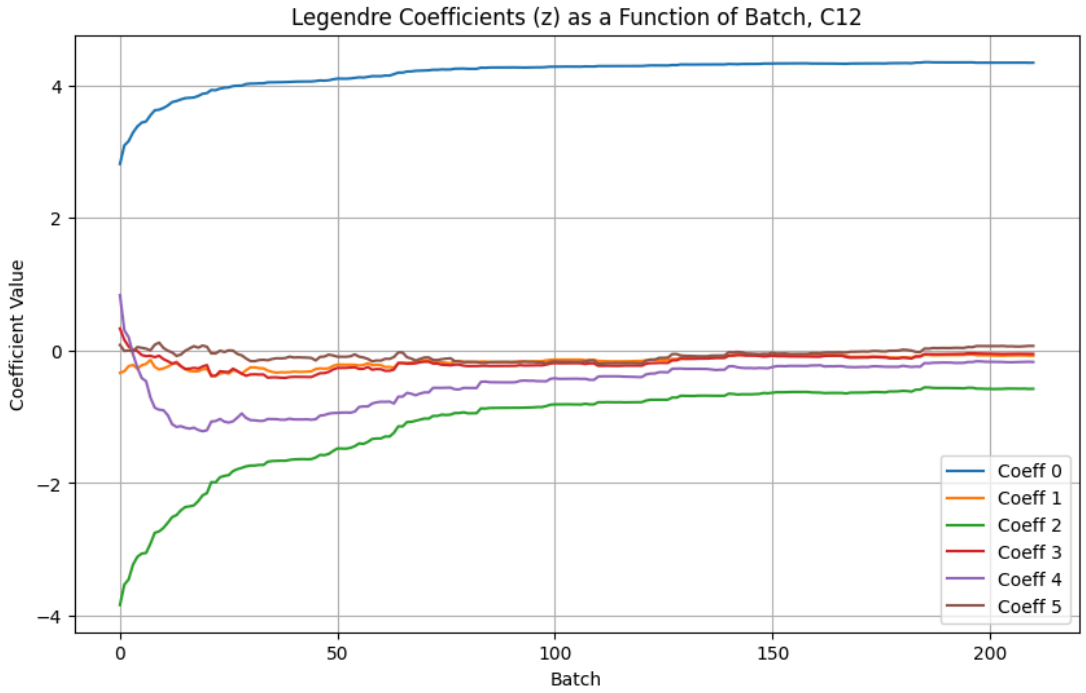

Figure 19. First six Legendre coefficients for ^{12}C effective cross section as a function of z

Table 2. Batch where coefficient n reached stationarity, by material

nth Coefficient	^{184}W	H_2O	^{12}C
0	86	91	40
1	48	71	25
2	146	158	91
3	95	96	36
4	146	152	33
5	46	52	35

The Legendre coefficients for H_2O and ^{184}W took much longer to converge than ^{12}C, likely owing to the complexity introduced by having either multiple atomic species to interact with, or the resonances present in a high-Z material.

The slowest-to-converge coefficient was the second-order Legendre coefficient for H_2O, which converged at batch 158 as opposed to 156 for the Shannon entropy case. Thus for this application, the stabilization of spatially-dependent energy on a fine, physically relevant timescale required roughly the same number of particles to be accumulated in the source bank as the stabilization of both spatially-dependent neutron density and energy on a much coarser level. Given that the accumulation of particles is a stochastic process, this difference is marginal and suggests good agreement between the two approaches. However, the reaction-rate based methodology may be preferable for some cases, as it does not necessitate a pre-defined mesh.

As an ultimate stationarity criteria, it was decided to consider the most conservative of these results: performing both the multi-dimensional Shannon entropy-based and effective cross section-based analysis of the surface source, and choosing the minimum batch count for accumulated particles to be 158. This particle and batch count was thus considered to be the minimum possible to be considered representative of the active core itself. Approaching this minimum conservatively, all of the neutrons banked on the surface source between the first and 250th active batch of the eigenvalue case were compiled into a single readable source file with a total of 9.2×10^5 total particles. Further evaluation of the effectiveness of this methodology, its limitations, and implications of oversampling the source were carried out by running OpenMC in fixed source mode with this created source file.

5. Evaluation of surface source banking

To evaluate the effectiveness of surface source banking as a technique for accelerating shielding and similar calculations in Monte Carlo codes, surface source files were compiled from neutrons banked as they crossed the surface source mesh during active batches of the eigenvalue case described in **Sec. 3.4**. A surface source file consisting of 250 active batches worth of particles (1.2×10^6 total particles) was compiled. Results from these fixed source cases were evaluated against results from a higher particle count eigenvalue case using a figure of merit metric that accounted for both uncertainty in spatial flux predictions and computational time. An additional eigenvalue case was run with 3×10^7 particles per batch to allow better simulation of far-field fluxes for comparison against fixed source cases, and otherwise had the same settings as the case described in **Sec. 3.4**. Potential causes for the limited discrepancies between the eigenvalue and fixed source results are also discussed.

5.1 Source bank use and figure of merit evaluation

To establish a means of directly comparing results, fixed source flux measurements were rescaled according to **Eq. 5**. In both cases, the neutron flux values plotted are the averaged neutron fluxes in 8x8x20 cm cells in a 2D cross section of the reactor geometry cutting through the z=0 midplane. To keep the scaling between results consistent, the active core region, where neutron fluxes are several orders of magnitude higher than the immediate surrounding regions, are capped at the highest average on the edge of the surface source.

An example of these results is shown in **Fig. 20**. For the fixed source results in **Fig. 20**, the surface source file from 250 batches worth of particles was utilized, with each particle in the bank simulated an average of once across all batches. As a note, the runtime of the fixed source case was 183s, and 10^5s for the longer eigenvalue case described in the previous section. **Fig. 21** shows the statistical error (error on flux, as calculated by OpenMC by each case divided by the flux magnitude) for each case.

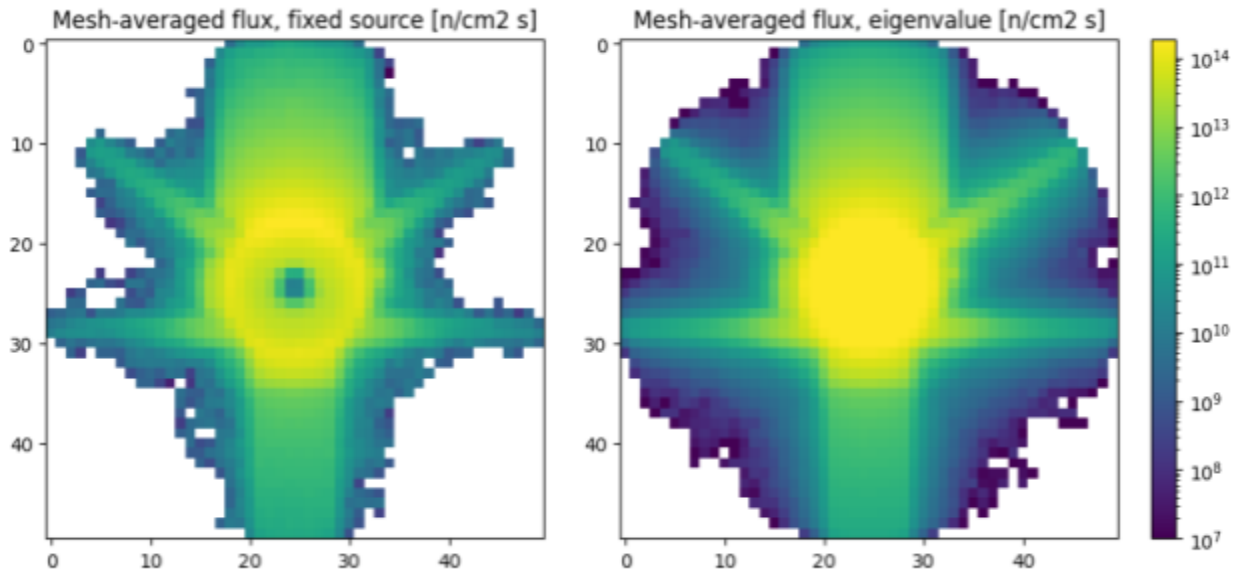

Figure 20. Mesh-averaged fluxes, fixed source and eigenvalue cases

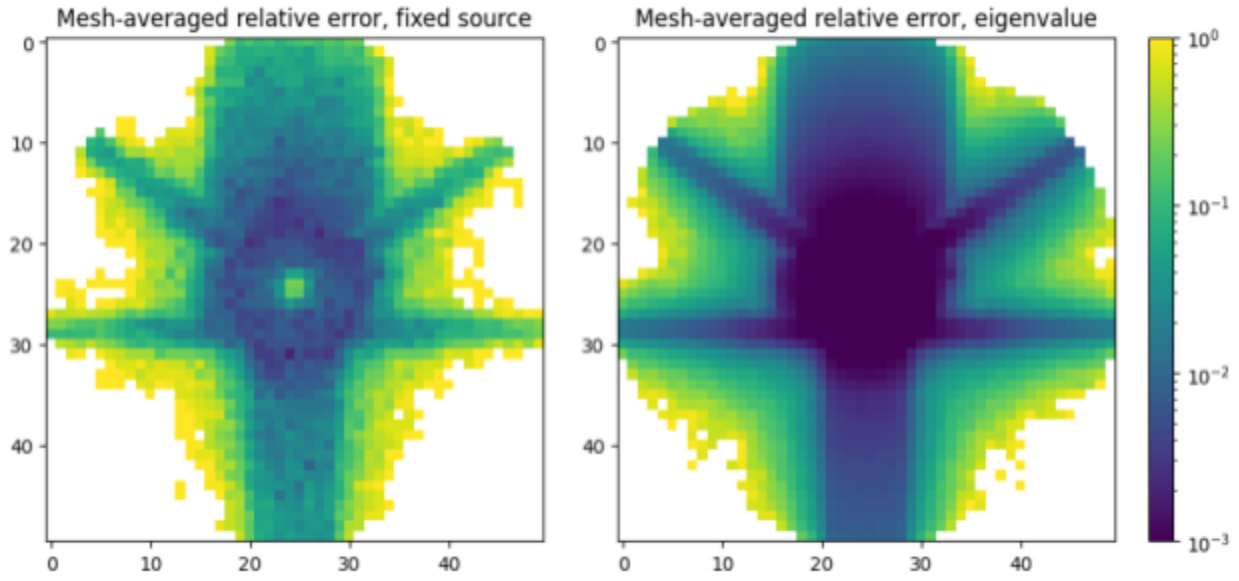

Figure 21. Mesh-averaged statistical error on fluxes, fixed source and eigenvalue cases

To better quantify the gains in computational efficiency from running fixed source simulations from a surface source bank, as opposed to eigenvalue cases, a figure of merit that accounts for both flux uncertainty and computation time (using the same resources for both cases). This figure of merit can be evaluated on a cell-by-cell basis for both the eigenvalue and fixed source cases via **Eq. 10**, where σ is the uncertainty, as returned by OpenMC (assuming particles are uncorrelated), on the averaged neutron flux in a mesh cell.

Equation 10. $\mathrm{FOM}_{\mathrm{cell}} = \dfrac{1}{\sigma^2_{\mathrm{cell}} \cdot t_{\mathrm{run}}}$

The cell-dependent ratio of FOM values between the fixed source and eigenvalue cases is shown in **Fig. 22**.

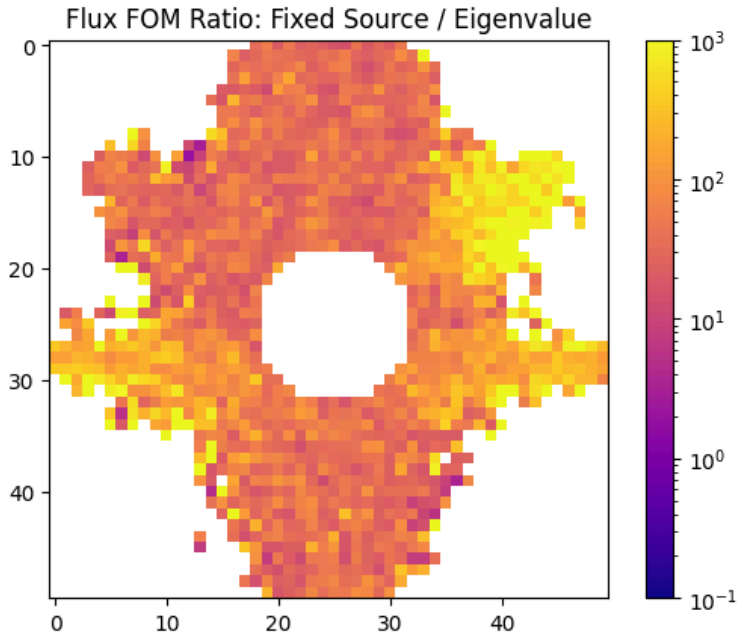

Figure 22. Figure of merit ratio: fixed source / eigenvalue

Excluding the active core region from consideration, the FOM ratio is almost universally greater than one in favor of the fixed source case, averaging at about 50 in most regions of the geometry. The FOM in and adjacent to the air-filled beam channels appears to be anomalously high—this is likely not a merit of the surface source banking technique itself, but rather a function of the physically narrow beam port entry regions right on the surface edge, and the high variance associated with evaluating flux via tallies in very low density areas. This effect can be seen more clearly by looking at the percent differences in particle fluxes between the eigenvalue and fixed source cases in **Fig. 23.**

Fig 23. shows that the fixed source case slightly over-predicts flux in the water tank and graphite columns, but significantly underpredicts flux in void-filled beam ports and adjacent regions. This effect is likely due to both the high variance associated with modeling flux in extremely low-density regions, as well as the surface source being placed directly adjacent to the beamport openings not capturing the sensitive "beam collimation" effect of the beamports that are effectively surrounded by neutron absorbing material. **Sec. 5.3** will further detail this effect and the limitations it may impose in very specific cases on surface source banking as a methodology. However, it appears that without oversampling the surface source, adequate flux

(and by extension, dose) predictions for non-void regions of the geometry can be established quickly via fixed source cases using a banked surface source that has been judged to have achieved stationarity via the means developed in this work.

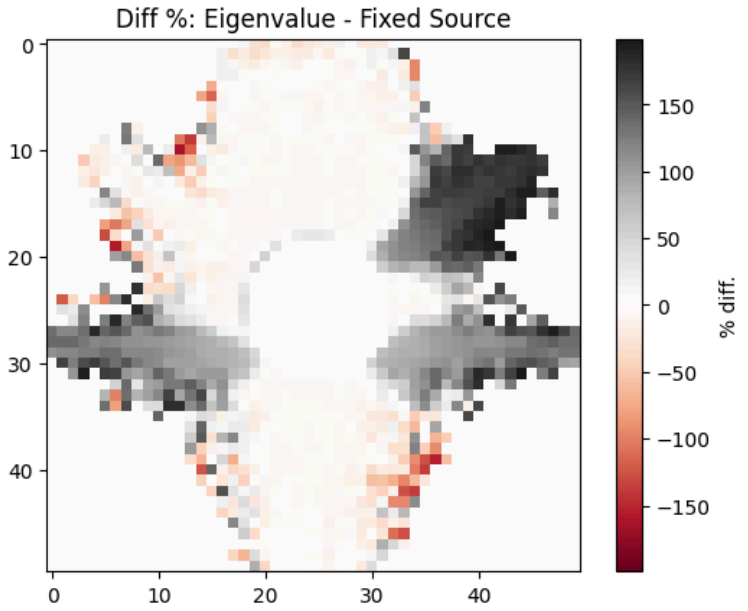

Figure 23. Percent difference in neutron flux, eigenvalue - fixed source

5.2 Oversampling effects

The previous section supports the utilization of surface source banking for gain in computational speed. However, as discussed in **Sec. 2.2**, a primary limitation on the approach is the need for a single extremely-high particle count eigenvalue run to produce a high-particle count surface source, and the size of the surface source file itself. Should the surface source be oversampled without introducing significant bias into the fixed source simulation results, this limitation becomes less significant.

In order to demonstrate this effect, the spatial statistical error on flux for the higher particle eigenvalue case was evaluated to determine which regions could reliably be used as a rough comparison against results from fixed source simulations. Mesh cell regions where statistical error was greater than 0.5, which are shown in red on **Fig. 24**, were removed from future comparisons against fixed-source results. This was done to minimize the risk of seeing accidental alignment between poorly-characterized eigenvalue and fixed source results. Two fixed source cases, one with each particle sampled an average of once from the surface source, and one with each particle sampled an average of one hundred times from the surface source were compared to the remaining results in the eigenvalue case.

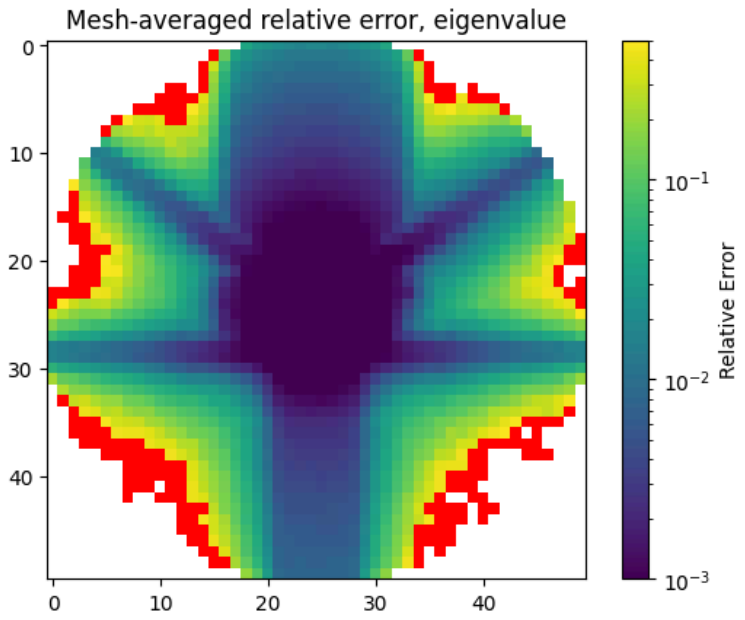

Figure 24. Statistical error on mesh-averaged flux, eigenvalue case

The results from both fixed source cases are compared to the eigenvalue case in **Fig. 25**. Outside of the radial beamport region (top right), which will be discussed in the following section, the percent difference between the results of both cases, despite significantly oversampling the surface source, does not appear more significant in the furthest-field regions simulated, which extend further than the case that was not oversampled. While this extreme case does not guarantee that bias and correlations introduced by oversampling have no negative impact on results, it suggests that oversampling a surface source judged by the criteria developed in **Sec 4.** to have reached stationarity can allow neutrons to be simulated quickly in regions of the core it would otherwise not reach.

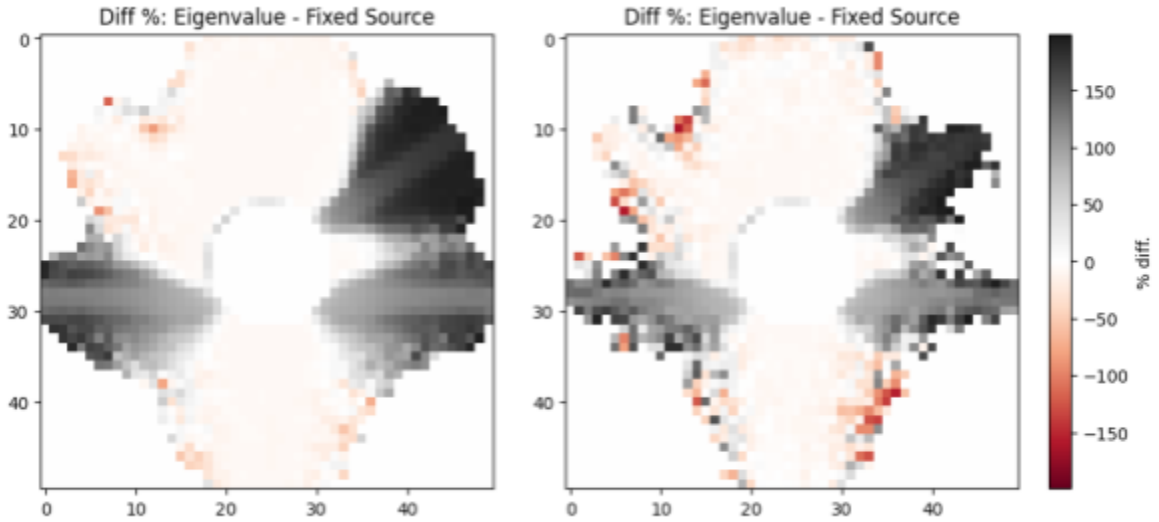

Figure 25. Left: x100 oversampled fixed source case, Right: each surface source particle simulated an average of once

The ability to simulate far-field flux in regions otherwise not reached without oversampling is demonstrated in **Fig 26**, comparing statistical error in flux between the eigenvalue case used for source banking (**Sec 3.4**) and oversampled fixed source case. Again, it must be noted that high-fidelity of the fixed source results would require establishing results in the far-field regions with adequate statistical error. However, given the lack of significant bias we see introduced by oversampling in the previous comparison of regions that can be verified against the eigenvalue, it is likely that these results are adequate for some use cases.

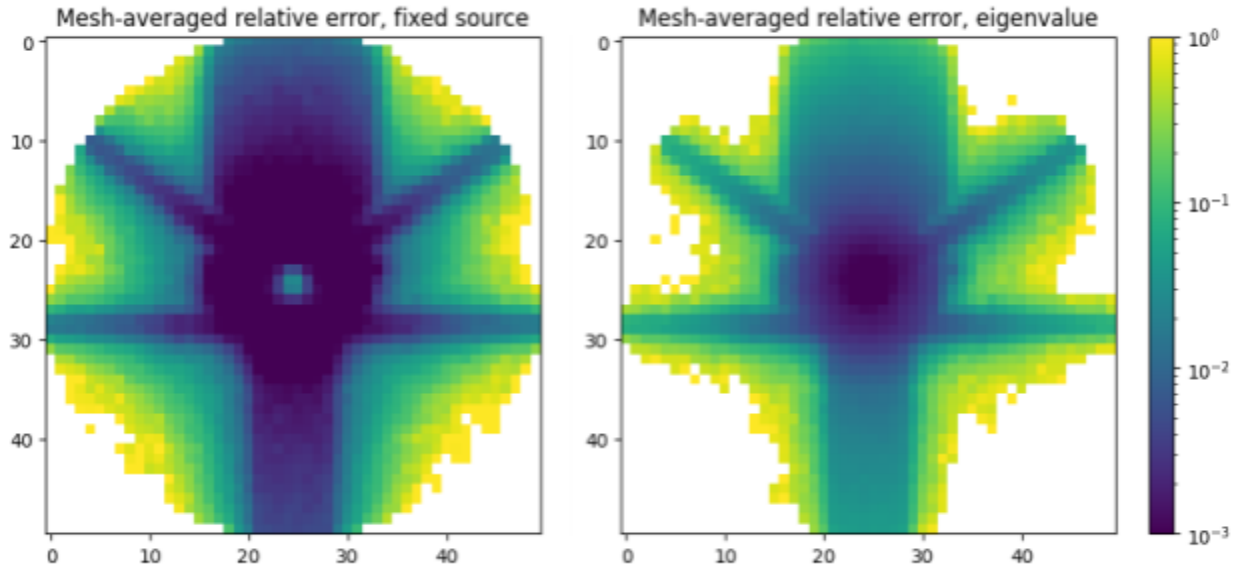

Figure 26. Statistical error on flux, Left: x100 oversampled case, Right: eigenvalue

5.3 Examining the beamport region discrepancies

A consistent discrepancy between the results of the eigenvalue and fixed source cases shown in the previous two sections is an under-prediction of neutron flux in the areas within and adjacent to MK2's air-filled beamports. Modeling of extremely low-density regions via Monte Carlo methods presents difficulties on its own, as the collisions that contribute to tallies are infrequent. Even when attempting to mitigate this issue via the use of track-length tallies, relative to all particles simulated, the behavior of neutrons within and adjacent to beamports is extremely sensitive to their trajectories—very few particles have a trajectory close enough to parallel with the beamport to travel more than a few cm without colliding with the outer wall and scattering into the surrounding concrete. As shown on **Fig. 27,** the region of greatest discrepancy between the eigenvalue and fixed source cases is the radial beamport, where the beamport opening is directly in contact with the surface source.

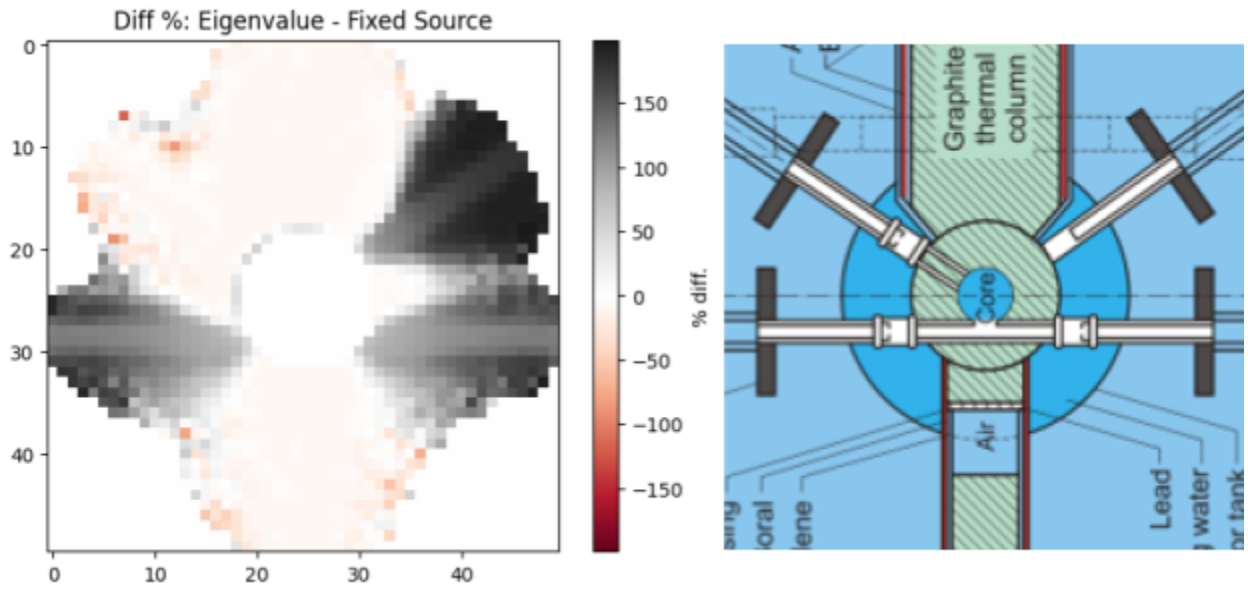

Figure 27. Flux magnitude discrepancies in relation to beamport geometry

An analysis of the neutron trajectories themselves offers more insight into these discrepancies and what might be done to resolve them for applying surface source banking to similar problems.

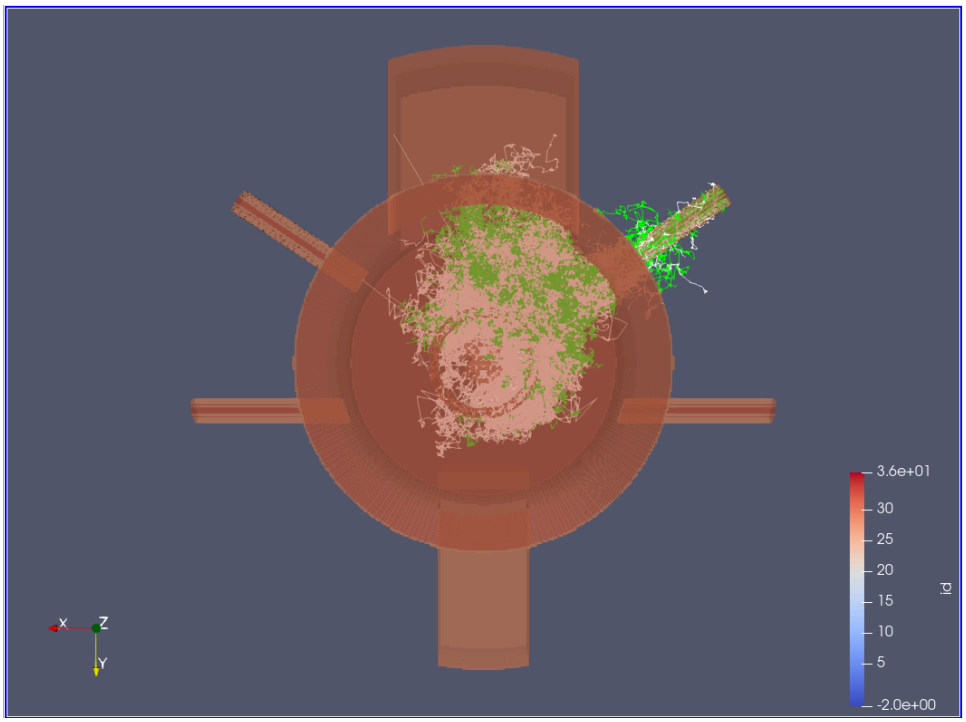

Figure 28: 3D voxel plot of the geometry with neutron trajectories overlaid

A low-particle count eigenvalue case, and a low-particle count fixed source case using the

surface source file from **Sec. 5.2** were run such that only the particle tracks of neutrons that entered the radial beamport (top left) could be recorded and compared between the two cases. Roughly three thousand particle tracks were recorded in each case, and plotted over a voxel plot of the geometry in **Fig. 27.** The concrete shield surrounding the core has been removed from the visualization so the particle tracks could be more easily seen. The fixed source particle tracks are in green, and the eigenvalue tracks are in white.

Looking closely at the particle tracks in **Fig. 29**, we see that the density of neutron tracks going "straight through" the beamport, as well as the amount of scatters into the concrete shield, are higher for the fixed source case. **Fig. 30** more closely shows this difference further down the beamport.

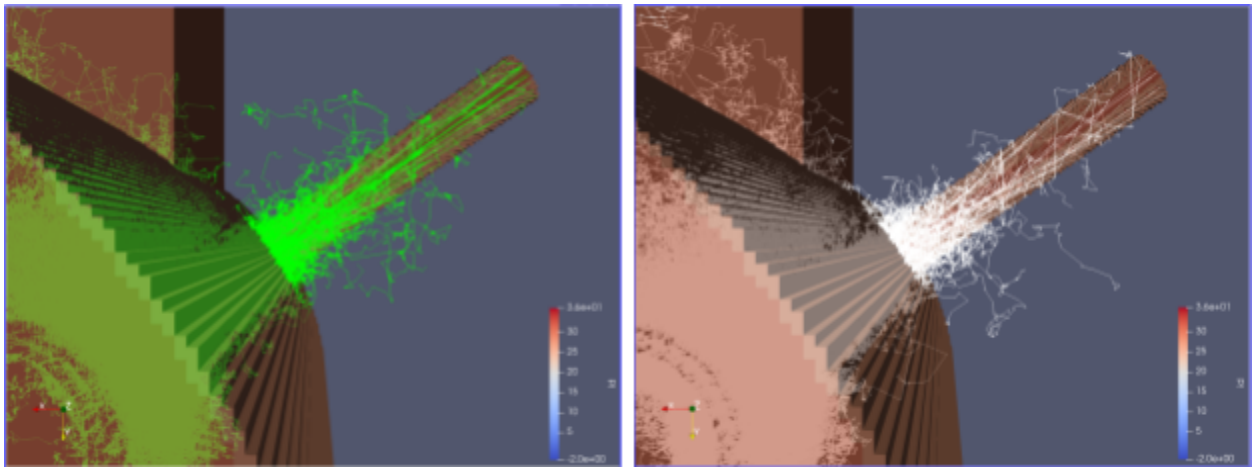

Figure 29. Neutron tracks through the radial beamport. Left: fixed source, Right: eigenvalue

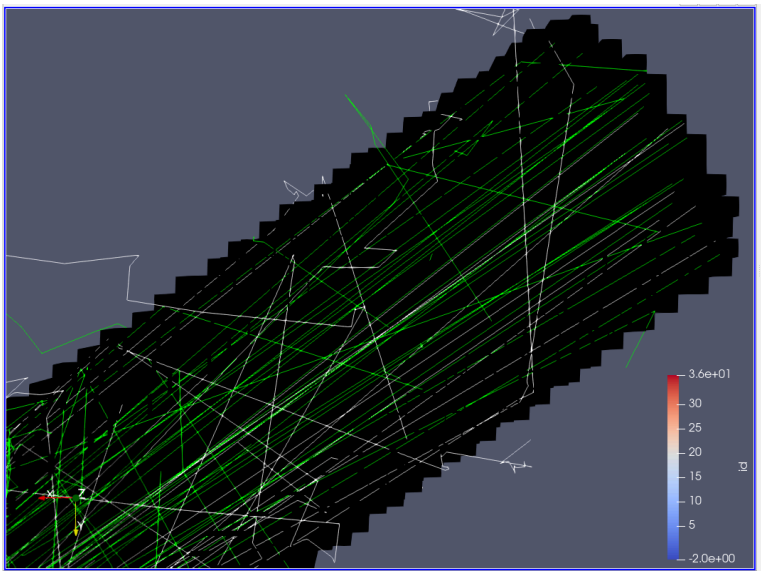

Figure 30. Close up view of particle track density at the far end of the radial beamport

These results likely visually confirm the need for much more in-depth verification of the angular distribution of the neutron flux for situations in which a void region is in contact with, or very close to the surface source mesh. Minor variations in the angular distribution of particles incident on a beamport that is effectively a beam collimator have significant effects on the far-downstream neutron flux, as well as in regions of the concrete shield where the main contributor to flux is neutrons scattering out of the beam. The lack of discrepancy in the piercing radial beamport (top left of **Fig. 27**) also supports this conclusion—the majority of the flux incident on this beamport opening enters from directly outside of the active core, having already been "collimated" by the beamport prior to being banked on the surface source. For the radial beamport, no beam collimation occurs upstream of the surface source, thus the trajectories of the neutrons incident on the surface must be exceptionally well defined to achieve well-matching results between the eigenvalue and fixed source cases.

It is not likely that this discrepancy is a function of correlations or oversampling of the surface source, as the total particle counts used for these simulations were several orders of magnitude smaller than the surface source bank used, owing to limitations from the memory-intensity of recording particle tracks.

To ensure that stationarity of the distribution of angular trajectories of neutrons incident on the portions of the surface source that open up into a beamport region is reached, particle trajectory would need to be added as an additional term to the Shannon entropy expression like shown in **Eq. 2**, or evaluated separately on an extremely fine mesh. More simply, the surface source could be positioned further downstream of the beam opening, and would likely significantly improve the issue, as can be seen with the piercing throughput. Another possibility is saving particle seeds in the surface bank data, such that their behavior through their entire history is identical to that of the eigenvalue case, which would eliminate the variation seen here. While this would reduce the variations between the cases, it would not indicate that a sufficiently converged surface source has been obtained. This suggestion will be discussed further in **Sec. 6.2**.

As shown in **Sec. 1**, regions outside of the beamports are well-modeled via the use of a surface source judged to have reached stationarity. More in-depth stationarity analysis can be carried out to avoid discrepancies when modeling beamport-like regions, but will require banking a larger number of particles. When utilized, surface source meshes should be placed downstream of beamport openings to avoid extreme sensitivity to variations in angular flux distributions, especially when relatively few neutrons compared to the total simulated enter the beamport.

6. Conclusions and Forward Work

6.1 Conclusions

In many situations, surface source banking could be a viable means of accelerating the inefficient simulation of far-field particle fluxes. However, the accuracy of the technique requires confidence that enough particles have been added to the source bank such that the source bank is adequately representative of an active core. In this work, two methods were developed and evaluated for making this determination. The first was adapted from existing approaches to determining the stationarity of fission source sites: tracking the batch-wise 2D Shannon entropy associated with the energy and position of particles cumulatively banked on a coarse mesh drawn over the banking surface. The second was continuously evaluating the Legendre coefficients associated with spatially-dependent effective reaction rates of the particles added to the source bank with a collection of different Z materials, and considering the surface source defined when the coefficients have converged within a predetermined tolerance. When tested with a surface source drawn on the edge of the graphite moderator ring on a model of a MK2 TRIGA reactor, both methods indicated that stationarity of the surface source was reached at the same number of banked particles. However, it is anticipated that the functional expansion method may be preferable for most use cases, as it is continuous and not affected by the choice of a mesh resolution to calculate entropy over.

A surface source was then compiled, and fixed source simulations using the surface source bank were conducted to determine the effectiveness and limitations of using what was determined to be a well-defined source bank. The figure-of-merit associated with using the surface source bank as opposed to an eigenvalue case to model far-field fluxes in the MK2 TRIGA was very favorable. It was also determined that oversampling a defined source enabled even faster simulation of further-field fluxes and did not introduce significant bias, but this investigation was limited in scope and should be repeated with better computational resources.

One potential limitation of surface source banking identified in this work is its ability to model narrow beamport-like regions, where relatively few neutrons enter a void region, and the survival of those neutrons is extremely sensitive to trajectory. The method's performance in scenarios where the surface source boundary is in contact with a beamport rather than downstream is limited if angular fluxes are not extremely well-defined on a fine spatial scale. This effect can be mitigated by repositioning of the surface source mesh, or potentially storing particle seeds in the source bank to exactly replicate particle histories between eigenvalue and surface-source cases.

Overall, now given a more robust means of determining surface source definition, the method has potential to reliably accelerate far-field flux simulations, which are especially of relevance in the fields of fusion energy and space nuclear technology.

6.2 OpenMC modifications required for surface banking viability

This work identified several means of improvement for OpenMC's surface source writing and reading capability. At present, OpenMC banks particles every time they cross a surface, resulting in some particles being banked multiple times. This is detrimental to the accuracy of fixed source simulations that use the surface source, as the energy spectrum of the surface source is significantly biased towards thermal neutrons that are more likely to "bounce back" and cross the surface multiple times. The magnitude of this effect is shown in **Fig. 31**.

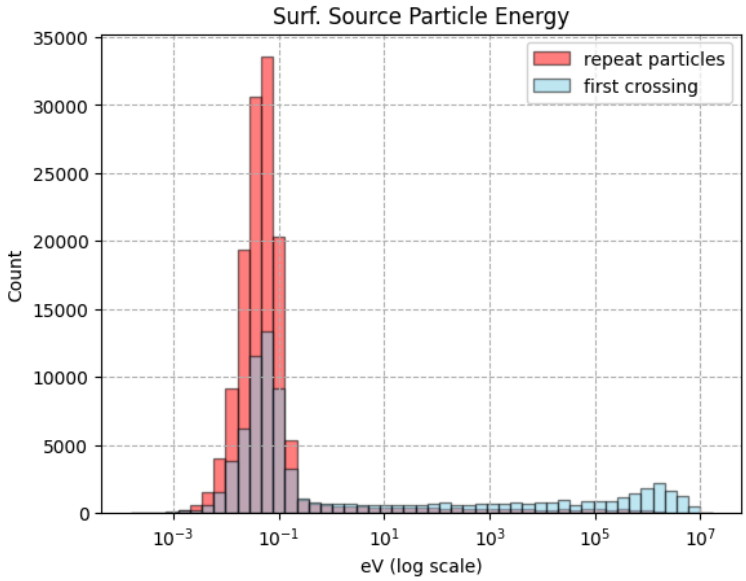

Figure 31. Impact of repeat surface crossings on surface source energy spectrum

Implementing a simple means of filtering the surface source particles by their id would resolve this issue for future versions of OpenMC. It is likely that this issue has gone unnoticed to date because the few uses of surface source banking in research have involved the placement of the banking surface far from active regions of the core, where the "bounce back" effect is minimized. This modification would also require redefining the source normalization factor that currently relies on current tallies impacted by these repeated crossings.

Additionally, the verification of surface source simulation results would be much more straightforward if there was an option to record particle seeds when reading and writing surface sources. While this would make oversampling of the surface source non-viable, having identical particle histories between eigenvalue and surface source-based cases would allow more reliable cross-verification in high-variance regions, such as the void-filled beamports discussed in **Sec. 5.3**.

6.3 Forward work to be explored

Presently, extremely little research on surface source banking is available. Further work should explore the overall effectiveness of the technique on reducing the computational load of a wider variety of problems. This work should involve further investigations of the effects of oversampling a surface source, and how the results might compare to that of very high particle count eigenvalue simulations where baseline far-field fluxes are known to a higher degree of confidence. It should also involve investigations of the best practices for using surface source banking on complex geometries that feature void regions, and some degree of particle collimation like that discussed in **Sec. 5.3**.

Additionally, future work should generally examine and further develop means of using Shannon entropy and functional expansions to evaluate the stationarity of surface source banks. The results of Shannon entropy-based evaluations of the source's stationarity are highly dependent on the resolution of the bins chosen to represent different aspects of the source—this dependency and effect on when stationarity of the source is indicated should be further investigated. A Shannon entropy-based means of evaluating spatially-dependent effective reaction rates was also conceived of during this work, but not investigated or compared to the functional expansion-based method. Given that the results of this work suggest the merit of utilizing Shannon entropy for evaluating surface sources, a more in-depth approach with effective reaction rates may be worth further exploring.

7. References

[1] P. K. Romano, N. E. Horelik, A. G. Nelson, B. Forget, and K. Smith, “OpenMC: A state-of-the-art Monte Carlo code for research and development,” *Ann. Nucl. Energy*, vol. 82, pp. 90–97, 2015.

[2] United States Executive Office of the President, “Executive order on promoting small modular reactors for national defense and space exploration,” Executive Order 13972, 86 FR 349, 2021.

[3] M. Nowak, A. M. G. Smith, B. Forget, and K. Smith, “Monte Carlo power iteration: Entropy and spatial correlations,” *Ann. Nucl. Energy*, vol. 94, pp. 856–867, 2016.

[4] F. Brown, “On the use of Shannon entropy of the fission distribution for assessing convergence of Monte Carlo criticality calculations,” in *Proc. PHYSOR-2006, ANS Topical Meeting on Reactor Physics*, Vancouver, BC, Canada, Sep. 10–14, 2006.

[5] Z. Han, “Performance analysis of functional expansion tallies on 2D PWR pin cell,” M.S. thesis, Dept. of Nuclear Science and Engineering, Massachusetts Institute of Technology, Cambridge, MA, 2020.

[6] U.S. Nuclear Regulatory Commission, “§ 36.25 Shielding,” *Code of Federal Regulations*, Title 10, Pt. 36, Aug. 29, 2017.

[7] S. Kumar, B. Forget, and K. Smith, “Stationarity diagnostics using functional expansion tallies,” *Ann. Nucl. Energy*, vol. 143, 107388, Aug. 2020.

[8] Massachusetts Institute of Technology, UChicago Argonne LLC, and OpenMC contributors, “8.3 Normalization of tally results,” *OpenMC Documentation*, version 0.15.2, 2025.

[9] Euro Labs, "JSI TRIGA Mark II reactor," 2025. All images and diagrams of the JSI MK2 TRIGA facility are taken from this webpage.